



3 8006 10039 0817

July 1965

The College of Aeronautics
Department of Aircraft Design.

OPTIMUM STRUCTURES

by

W.S. Hemp

H.S.Y. Chan

Report of contract work sponsored by the
Machine Tool Industry Research Association.



Contents

	<u>Page</u>
<u>Introduction</u>	1
<u>Section 1</u> Frameworks	2
<u>Section 2</u> Michell Type Theorem for Reinforced Plate.	6
<u>Section 3</u> Analysis of the Virtual Deformation in Two-Dimensions.	8
<u>Section 4</u> Examples of Virtual Deformation	11
<u>Section 5</u> Conditions of Equilibrium	17
<u>Section 6</u> First Example of a Force Reacted at Two Fixed Supports. (Case when Force is Normal to the Line of Supports)	19
<u>Section 7</u> Second Example of a Force Reacted at Two Fixed Points. (Case when Force is Parallel to the Line of Supports)	22
<u>Section 8</u> Examples of the Determination of Volumes, Plate Thicknesses and Reinforcing Member Sizes.	24
<u>Section 9</u> Method of Approximate Numerical Analysis.	31
<u>Section 10</u> Future Developments.	34
<u>References</u>	36
<u>Appendix A</u> Detailed Analysis of Figure 7.	37
<u>Appendix B</u> Analytical Method for Integrating the Hyperbolic Differential Equations	40
<u>Figures</u>	

Optimum Structures

Introduction

The design of the best structure for a given purpose depends upon the criterion used for optimisation. Structures may be designed to safely transmit a given system of forces using the least weight of material. They may also be designed to have maximum stiffness of a certain type for a given weight or alternatively to have the greatest possible fundamental frequency of vibration. These problems, although in general distinct from one another, are closely related and much can be achieved towards maximisation of stiffness and frequency by the use of minimum weight designs. In fact it can be shown that a minimum weight framework is the stiffest structure of that weight for the force system, which it is designed to carry.*

The present report is concerned exclusively with the problem of the design of structures of minimum weight, which are required to transmit specified forces. Some attention will be given to frameworks because, in particular, methods of approximate numerical analysis are more readily formulated for this type of structure, but the main emphasis will be placed upon the design of structures formed from plates of variable thickness reinforced by direct load carrying members.

* See para.1.4

Section 1. Frameworks

1.1 The problem of designing the lightest framework which will equilibrate a system of given forces was first considered by A.G.M. Michell (Ref.1). Structures designed according to his principles are therefore called 'Michell structures'.

1.2 Consider any system of forces in equilibrium F , with their points of action contained in a region R of space, within which a structure, which equilibrates them, is required to lie. (Fig.1) The system F can be balanced by an infinite variety of pin-jointed structures S , lying in R , and made from a material capable of carrying stresses $\pm f$ ($f > 0$) in tension and compression respectively. If T is the end load in any member of any S with cross-section area A , then

$$|T| \leq fA . \quad \dots (1.1)$$

Impose a virtual deformation D on the region R , restricted so that the change in length L of any linear segment of length L in R satisfies

$$|\Delta L| \leq eL , \quad \dots (1.2)$$

where e is a positive infinitesimal. Let W be the virtual work of F taken over the displacements of D . This will be equal to the 'internal' virtual work in any of the structures S and so

$$W = \sum T \Delta L \quad \dots (1.3)$$

where ΔL applies here to a number of S and \sum sums over all members of S .

Equation (1.3), using (1.1) and (1.2), then implies

$$|W| = \left| \sum T \Delta L \right| \leq \sum |T| |\Delta L| \leq f_e \sum AL = f_e V$$

where V is the volume of material contained in the structure S . It follows that, for any V of S and any D satisfying (1.2),

$$V \geq \frac{|W|}{f_e} \quad \dots (1.4)$$

Picking out that D which makes $|W|$ a maximum then implies

$$V \geq V_m \quad \dots (1.5)$$

where

$$V_m = \frac{|W|_{\max}}{f_e} \quad \dots (1.6)$$

The quantity V_m is thus a lower bound to the volumes of all structures S which equilibrate the given forces.

1.3 The argument of para.1.2 does not show that there is a structure S_m with volume V_m . The existence of such a structure has been shown in many special cases, but no general proof is known. A Michell structure S_m is characterised by

$$|T| = fA \quad \dots (1.7)$$

and by the existence of a D_m satisfying

$$|\Delta L| = eL \quad \dots (1.8)$$

for all its members and such that the sign of ΔL agrees with that of T for all the members of S_m . Equations (1.3), (1.7) and (1.8) then show that $W = f_e V$ for a Michell structure and so by (1.6) its volume is $\leq V_m$. It must also satisfy (1.5) and hence its volume is precisely V_m . A Michell structure, if it exists, is thus the lightest possible structure which equilibrates the given forces.

1.4 A Michell structure is also the stiffest structure among all the frameworks of volume V_m , which are able to transmit the given forces F . The proof of this result falls into two parts. In the first place a structure of given layout is considered and that distribution of cross-sectional areas A is sought such that, for constant total volume $V = \sum AL$, the work done U by given forces F is as small as possible. If w is the displacement corresponding to F and ϵ the strain in a member, whose material has modulus E then U is given by

$$U = \frac{1}{2} Fw = \sum \left(\frac{1}{2} E \epsilon^2 \right) AL \quad \dots (1.9)$$

Consider then a variation δA of A and let δw , $\delta \epsilon$ be the consequent changes in w and ϵ . The condition for minimum U is then

$$\delta U = \frac{1}{2} F \delta w = \sum \left\{ \delta \left(\frac{1}{2} E \epsilon^2 \right) AL + \left(\frac{1}{2} E \epsilon^2 \right) \delta AL \right\} = 0 \quad \dots (1.10)$$

where the δA are restricted by the constancy of V to satisfy

$$\sum \delta AL = 0 \quad \dots (1.11)$$

Now the deformation characterised by δw , $\delta \epsilon$ may be taken as a virtual deformation for the unvaried structure which is in equilibrium under F . It follows therefore that

$$F \delta w = \sum \delta \left(\frac{1}{2} E \epsilon^2 \right) AL \quad \dots (1.12)$$

and that the condition (1.10) implies

$$\sum \left(\frac{1}{2} E \epsilon^2 \right) \delta AL = 0 \quad \dots (1.13)$$

Combining (1.13) with (1.11), introducing a constant Lagrangian multiplier λ , then gives

$$\sum \left\{ \frac{1}{2} E \epsilon^2 - \lambda \right\} \delta AL = 0$$

from which it may be concluded that *

$$\frac{1}{2} E e^2 = \lambda \quad \dots (1.14)$$

or that the strain energy density and in consequence the numerical values of the strain and the stress are constant for all members of the structure.

Consider now, in the second place, structures which transmit the forces F with constant stresses $\pm f$ in all their members. The total strain energy in such a structure is $(f^2/2E)V$ and this reaches its minimum value when $V = V_m$, i.e. when it is a Michell structure. It has thus been demonstrated that a Michell framework is the stiffest structure among those of volume V_m .

1.5 The virtual deformation D_m associated with a Michell framework must satisfy (1.2) in R and (1.8) along lines, which are the layout lines of the structure. The simplest deformation of this kind is a uniform dilatation of space with linear strain e (or $-e$). In this case all lines have the strain e (or $-e$) and no restriction is imposed on layout. However all members must carry tension (or compression) loads and so a rather specialised, but nevertheless important class of structures results. Any structure which can carry forces F by means of members which all have stress f (or $-f$) is an optimum structure and all such structures have the same weight, independently of their layout.

A second kind of deformation D_m , appropriate to two-dimensional structures, is that for which the values of the principal strains are $\pm e$. The principal strain lines are then possible layout lines for Michell structures. It can then be shown, as in Section 3 below, that compatibility of

* The values of A are restricted by $A \geq 0$. If the best value of U requires some members to have zero areas, then these can be omitted from the summation Σ .

strain imposes geometrical restrictions on these layout lines, which are the same as those satisfied by the slip lines in perfect plastic flow. They must in fact satisfy Hencky's theorems (Ref.2, Chap.VI,4) and this immediately provides methods for their construction. This analogue with plastic flow has been exploited in for example Refs. 3, 4 and 5.

Very little is known about layout lines in three-dimensions. Michell gave in Ref.1 a structure for the transmission of torsion consisting of members lying along the rhumb lines on a sphere. Other optimum structures have been obtained by rotating two-dimensional layouts. However no general theory has as yet been developed.

Section 2. Michell Type Theorem for Reinforced Plates

2.1 The present section deals with the principles governing the optimum design of reinforced plates P, lying in a region R of a plane, which safely equilibrate a given system of forces F or safely transmit these forces to a rigid support \mathcal{S} . (see Fig.2). The plates are assumed capable of carrying membrane stresses, with principal values f_1 and f_2 and the reinforcing members of carrying direct stresses f_R . The safety of the designs is ensured by imposing the Tresca yielding criterion:

$$\left. \begin{array}{l} \text{Maximum difference between } f_1, f_2, 0 \leq f \\ \text{and } |f_R| \leq f \end{array} \right\} \dots (2.1)$$

where f is the yield stress in tension.*

* The plates P are designed in accordance with the philosophy of 'limit design'.

2.2 Let it be assumed that a plate P^* can be formed, which satisfies

$$\left. \begin{aligned} &\text{Maximum difference between } f_1^*, f_2^*, 0 = f \\ &\text{and } |f_R| = f \end{aligned} \right\} \dots (2.2)$$

and is such that a virtual deformation D of the region R exists with principal strains e_1 and e_2 , lying in the same directions as f_1^* and f_2^* , and with magnitudes

$$\left. \begin{aligned} e_1 &= +e, \quad e_2 = -e \quad \text{in region } R_1, \text{ where } f_1^* - f_2^* = +f \\ e_1 &= +e, \quad e_2 = 0 \quad \text{in region } R_2, \text{ where } f_1^* = +f \\ e_1 &= 0, \quad e_2 = +e \quad \text{in region } R_3, \text{ where } f_2^* = +f \end{aligned} \right\} \dots (2.3)$$

and which further has strains $+e$ along reinforcing members with stresses $f_R = +f$. The quantity e is a positive infinitesimal constant and the deformation D is assumed to be produced by conventional 'small' displacements. These displacements are assumed to vanish on \mathcal{A} . It will be shown in para.2.3 that such a plate P^* , if it exists, is an optimum design among all plates P and since its specification in (2.2) and (2.3) is of the same form as that of equations (1.7) (1.8) it may be termed a Michell plate.

2.3 Let W be the virtual work of the forces F taken over the displacements of D. If f_{11} , f_{22} and f_{12} are the membrane stresses in a P referred to the directions of e_1 and e_2 and e the virtual strain along a reinforcing member then

$$W = \int t_p (f_{11}e_1 + f_{22}e_2) dS + \sum \int A_R f_R e ds \quad \dots (2.4)$$

where t_p is the thickness of the plate, A_R the cross-sectional area of a reinforcing member with arc length s , \sum a sum over all reinforcing members and dS an element of plate area.

* It is to be remembered that a case such as $f_2^* = 0$ can be included in either R_1 or R_2 .

In the case of the Michell plate P^* , (2.2), (2.3) show that (2.4) can be written

$$W = \int_R t_p^* f e dS + \sum \int A_R^* f e dS = f e V^* \quad \dots (2.5)$$

where V^* is the volume of the material of P^* .

Equations (2.4) (2.5) yield the inequality

$$\begin{aligned} f e V^* &\leq \int_R t_p \left| f_{11} e_1 + f_{22} e_2 \right| dS + \sum A_R \left| f_R \right| \left| \epsilon \right| dS \\ &\leq \int_{R_1} t_{pe} \left| f_{11} - f_{22} \right| dS + \int_{R_2} t_{pe} \left| f_{11} \right| dS + \int_{R_3} t_{pe} \left| f_{22} \right| dS \\ &\quad + \sum \int A_R e \left| f_R \right| dS \end{aligned}$$

when (2.3) has been used, and so, since $(f_{11} - f_{22})^2 + 4f_{12}^2 \leq f^2$ by (2.1) and $|f_{11}|$, $|f_{22}|$ are both less than or equal to the greatest of $|f_1|$, $|f_2|$ it follows by (2.1) that,

$$f e V^* \leq \int_R t_p e f dS + \sum A_R e f dS = f e V$$

where V is the volume of material in P . It has been established that

$$V \geq V^* \quad \dots (2.6)$$

and so P^* is the lightest plate structure which will safely carry the given forces F . Its volume can be calculated from (2.5), when the associated virtual deformation D is known.

Section 3. Analysis of the Virtual Deformation in Two Dimensions

3.1 The lines of principal strain of a virtual strain system D , as defined in Section 2, may be used to define an orthogonal system of curvilinear coordinates (α, β) , which are to be taken as right-handed with the strain e_1 along the α -lines and e_2 along the β -lines. The linear element ds is given by

$$ds^2 = A^2 d\alpha^2 + B^2 d\beta^2 \quad \dots (3.1)$$

where A, B are positive functions of α, β . The angle ϕ between the tangent to an α -line in the direction of α increasing and a reference line, the x-axis of a Cartesian system $O(x,y)$, which is shown in Fig.3, is related to A,B by

$$\frac{\partial \phi}{\partial \alpha} = -\frac{1}{B} \frac{\partial A}{\partial \beta}, \quad \frac{\partial \phi}{\partial \beta} = \frac{1}{A} \frac{\partial B}{\partial \alpha} \quad \dots (3.2)$$

The relation between the coordinates x,y and α,β is given by

$$x + iy = x_0 + iy_0 + \int_{(0,0)}^{(\alpha,\beta)} (A d\alpha + iB d\beta) \exp(i\phi) \quad \dots (3.3)$$

where (x_0, y_0) corresponds to $\alpha = \beta = 0$. The equations (3.2) ensure the uniqueness of the integral in (3.3), which follows, using (3.1), from the standard formulae for direction cosines of the tangent to a curve.

3.2 Let the displacements in the directions of α, β increasing be u, v . The direct strains in the α, β directions have the constant values e_1, e_2 while the corresponding shear strain is zero. Denoting the 'rotation' by ω , the standard formulae for curvilinear coordinates (Ref.6, Chap.I, equations (36) and (38)) give

$$\left. \begin{aligned} \frac{1}{A} \frac{\partial u}{\partial \alpha} - \frac{v}{A} \frac{\partial \phi}{\partial \alpha} &= e_1, & \frac{1}{B} \frac{\partial v}{\partial \beta} + \frac{u}{B} \frac{\partial \phi}{\partial \beta} &= e_2 \\ \frac{1}{A} \frac{\partial v}{\partial \alpha} + \frac{1}{B} \frac{\partial u}{\partial \beta} + \frac{u}{A} \frac{\partial \phi}{\partial \alpha} - \frac{v}{B} \frac{\partial \phi}{\partial \beta} &= 0 \\ \frac{1}{A} \frac{\partial v}{\partial \alpha} - \frac{1}{B} \frac{\partial u}{\partial \beta} + \frac{u}{A} \frac{\partial \phi}{\partial \alpha} + \frac{v}{B} \frac{\partial \phi}{\partial \beta} &= 2\omega \end{aligned} \right\} \quad \dots (3.4)$$

The solution of (3.4) for the derivatives of u, v gives, in differential form,

$$d(u + iv) = (Ae_1 d\alpha + iBe_2 d\beta) + i\omega(A d\alpha + iB d\beta) - i(u + iv)d\phi \quad \dots (3.5)$$

The condition that (3.5) is a total differential, yields on using (3.2), the relations

$$\frac{\partial \omega}{\partial \alpha} = (e_1 - e_2) \frac{\partial \phi}{\partial \alpha}, \quad \frac{\partial \omega}{\partial \beta} = -(e_1 - e_2) \frac{\partial \phi}{\partial \beta} \quad \dots (3.6)$$

which can also be written as

$$\left. \begin{aligned} \omega - (e_1 - e_2)\phi &= \text{constant on an } \alpha\text{-line} \\ \omega + (e_1 - e_2)\phi &= \text{constant on a } \beta\text{-line} \end{aligned} \right\} \quad \dots (3.7)$$

Finally the consistency of (3.6) yields, since $e_1 \neq e_2$,

$$\frac{\partial^2 \phi}{\partial \alpha \partial \beta} = 0 \quad \dots (3.8)$$

3.3

The result given in (3.8) shows that the lines of principal strain of D , which are the α, β coordinate lines, satisfy the same geometrical theorems, the theorems of Hencky, as are satisfied by the slip lines in two-dimensional plastic flow. The analytical and graphical methods given in, for example, Ref.2 for the construction of slip lines can then be used for the solution of the present problem of finding virtual deformation fields D .

The α, β lines can also be used as layout lines for two-dimensional Michell frameworks. This follows since the associated virtual strain fields for frameworks, which contain both tension and compression members, are a special case of the general investigation of this section obtained by writing $e_1 = \bar{t}e$, $e_2 = \bar{r}e$.



3.4 The conditions to be satisfied at a line of rigid support \mathcal{L} can be obtained from (3.5), by writing $u + iv = 0$. This gives

$$\omega = \frac{1}{2}(-e_1 e_2)^{1/2}, \quad A e_1^{1/2} d\alpha + B(-e_2)^{1/2} d\beta = 0 \dots (3.9)$$

and this implies that ω is constant along \mathcal{L} and that the coordinate lines meet \mathcal{L} at constant angles. For the region R_1 the angle is $\pi/4$ and for R_2 and R_3 either 0 or $\pi/2$.

Section 4. Examples of Virtual Deformation

4.1 The simplest example of a virtual strain field is obtained by taking α, β to be rectangular Cartesian coordinates. For these $A = B = 1$ and so by equation (3.2) ϕ equals a constant. Equation (3.3) then gives

$$\left. \begin{aligned} x &= x_0 + \alpha \cos\phi - \beta \sin\phi \\ y &= y_0 + \alpha \sin\phi + \beta \cos\phi \end{aligned} \right\} \dots (4.1)$$

which shows that the origin of the (α, β) system is at (x_0, y_0) and that the α -lines are inclined at an angle ϕ to the x-axis (Fig.4).

Equation (3.6) shows that $\omega = \text{constant}$ and equation (3.5) integrates to give

$$\left. \begin{aligned} u &= u_0 - \omega\beta + e_1\alpha \\ v &= v_0 + \omega\alpha + e_2\beta \end{aligned} \right\} \dots (4.2)$$

4.2 A second example is obtained by taking (α, β) to be polar coordinates with $A = 1$ and $B = \alpha$. Equation (3.2) now gives

$$\phi = \beta + \phi_0 \dots (4.3)$$

and (3.3) yields

$$\left. \begin{aligned} x &= x_0 + \alpha \cos(\beta + \phi_0) \\ y &= y_0 + \alpha \sin(\beta + \phi_0) \end{aligned} \right\} \dots (4.4)$$

This coordinate system is shown in Fig.5.

Equation (3.6) gives

$$\omega = -(e_1 - e_2)\beta + \omega_0 \quad \dots (4.5)$$

which implies, since β and $\beta + 2\pi$ gives the same radius vector, that this deformation field must be restricted to a range of β less than or equal to 2π . Equation (3.5) integrates^{*} to give

$$\left. \begin{aligned} u &= C_1 \cos\beta + C_2 \sin\beta + e_1 \alpha \\ v &= -C_1 \sin\beta + C_2 \cos\beta + \omega_0 \alpha - (e_1 - e_2)\alpha\beta \end{aligned} \right\} \quad \dots (4.6)$$

where (C_1, C_2) is the displacement of the origin of the (α, β) system resolved along the reference line and its normal.

4.3

The fields of para.4.1 and para.4.2 may be combined together to give the field illustrated in Fig.6. In the region OAA' the radii have strains e_1 and the circles strains e_2 . The opposite is true in the region OBB'. The regions OBCA and OB'C'A' have rectilinear principal strain lines with matching values of strain with those in quadrants, which they meet along OA, OB, OA' and OB'. The origin O may be assumed to be at rest and the field may be taken to be symmetrical about the bisector of the angles AOA' and BOB'. This implies by (4.5) that the rotation of OA is $(e_1 - e_2)\pi/4$. This is shown in the figure, as are the corresponding rotations of OA', OB and OB'. It is clear that continuity of displacement can be achieved at the joins between the several regions by giving the rectangles OBCA and OB'C'A' opposing rotations of magnitude $(e_1 - e_2)\pi/4$. It is to be remarked that the field of Fig.6 can be extended over the whole plane, since there is no restriction on the length of OA.

* This integration may be checked by (3.4)

4.4 In the combined field of Fig.6 the angles AOA' , BOB' are right angles. A variant in which these angles are less than a right angle, (say) 2θ , is shown in Fig.7. The rotations of the lines OA , OA' , OB , OB' and of the squares $OACB_1$, $OA'C'B'_1$, are now $(e_1 - e_2)\theta$ and in fact a consistent displacement field valid for the whole plane can be constructed assuming that the regions OBB_1 , $OB'B'_1$ are in a state of hydrostatic strain with a linear strain equal to e_2^{\equiv} . The optimum structures cannot of course lie in these last regions, since the strains there are inconsistent with (2.3). However the rest of the plane may be used^{*} and while it does not lead to absolute optima, it gives optimum structures for the case where OBB_1 and $OB'B'_1$ are excluded.

4.5 If one of the α (or β) coordinate lines is a straight line then all the other coordinate lines of this system are also straight lines. This follows from (3.8), which has the general integral $\phi = F_1(\alpha) + F_2(\beta)$, where F_1 and F_2 are arbitrary functions. If ϕ is constant for any particular β then F_1 is a constant and so ϕ is constant along every α -line.

In the case where the α -lines are straight they will in general envelop an evolute curve[†] and the β -lines will then be the corresponding involutes. The distance along the α -lines between any pair of evolutes is then a constant and the coordinate α may therefore be taken to be such a distance measured from a fixed involute $\alpha = 0$. The coordinate β may be taken as the angle between an α -line and a fixed direction. The distance, measured along an α -line, from a point on $\alpha = 0$ to the evolute will then be a function of β , say $F(\beta)$

[≡] A detailed analysis is given in Appendix A.

^{*} The complete plane is available for a framework or for reinforced plates in which only reinforcing members lie in the regions of hydrostatic strain.

[†] This may degenerate to a point to give the case of para.4.2.

and then as may be seen from Fig.8 the values of A, B and ϕ are

$$A = 1, \quad B = \alpha + F(\beta), \quad \phi = \beta \quad \dots (4.7)$$

Equation (3.3) gives

$$x + iy = x_0 + iy_0 + \alpha \exp(i\beta) + i \int_0^\beta \exp(i\beta)F(\beta)d\beta \quad \dots (4.8)$$

and (3.6) yields

$$\omega = \omega_0 - (e_1 - e_2)\beta \quad \dots (4.9)$$

where ω_0 is a constant. Finally (3.5) integrates to give

$$\begin{aligned} u + iv = & (u_0 + iv_0)\exp(-i\beta) + \left[e_1 + i \{ \omega_0 - (e_1 - e_2)\beta \} \right] \alpha \\ & + \exp(-i\beta) \int_0^\beta \{ ie_2 - \omega_0 + (e_1 - e_2)\beta \} \exp(i\beta)F(\beta)d\beta \quad \dots (4.10) \end{aligned}$$

4.6

An important development of Fig.6 is shown in Fig.9. The discussion in para.4.3 shows that a consistent displacement field can be found for the region shown with the points O and C taken at rest. The question then arises as to whether the lines of constant strain e_1 and e_2 can be extended into the rest of the plane. The analogy with slip lines in plastic flow shows that this is indeed possible beginning with the orthogonal circles AA' and AA'' or with BB' and BB''. * Fig.10 shows the general form of the layout and defines an appropriate coordinate system in which AA'' and AA' are 'coordinate axes' and the coordinates (α, β) are determined by the angles through which the tangents to AA'', AA' respectively turn as their points of contact advance along these circles.

* Ref.2, Chap.VI.

If the reference direction $\phi = 0$ is taken as the direction of the tangent to AA'' at A then $\phi = -\alpha$ on AA'' or $\beta = 0$ and $\phi = \beta$ on AA' or $\alpha = 0$. Equations (3.7) then give, taking ω_0 as the value of ω at A,

$$\omega_0 = \omega(\alpha, 0) - (e_1 - e_2)(-\alpha)$$

$$\omega_0 = \omega(0, \beta) + (e_1 - e_2)\beta$$

$$\omega(0, \beta) - (e_1 - e_2)\beta = \omega(\alpha, \beta) - (e_1 - e_2)\phi(\alpha, \beta)$$

$$\omega(\alpha, 0) + (e_1 - e_2)(-\alpha) = \omega(\alpha, \beta) + (e_1 - e_2)\phi(\alpha, \beta)$$

It follows that

$$\phi = -\alpha + \beta \quad \dots (4.11)$$

$$\text{and } \omega = \omega_0 - (e_1 - e_2)(\alpha + \beta). \quad \dots (4.12)$$

Equations (3.2) then give

$$\frac{\partial A}{\partial \beta} = B \quad \text{and} \quad \frac{\partial B}{\partial \alpha} = A \quad \dots (4.13)$$

and an appropriate solution of these equations, ^{*} which satisfies the initial conditions $(A)_{\beta=0} = (B)_{\alpha=0} = R$ is given by

$$\left. \begin{aligned} A(\alpha, \beta) &= R \left\{ I_0(2\sqrt{\alpha\beta}) + \sqrt{\frac{\beta}{\alpha}} I_1(2\sqrt{\alpha\beta}) \right\} \\ B(\alpha, \beta) &= A(\beta, \alpha) \end{aligned} \right\} \quad \dots (4.14)$$

where I_0 and I_1 are modified Bessel functions of zero and first order respectively.

Formulae may also be obtained from (3.3) and (3.5) for the cartesian coordinates (x_1, y_1) and for the displacements (u_1, v_1) in the region $AA''DA'$.

^{*} See Appendix B

It is found from Ref.7, Eq.(17),(18), that

$$\begin{aligned} u_1(\alpha, \beta) &= e_1 R \{ (1+2\alpha) I_0(2\sqrt{\alpha\beta}) + 2\sqrt{\alpha\beta} I_1(2\sqrt{\alpha\beta}) \} \\ v_1(\alpha, \beta) &= e_2 R \{ (1+2\beta) I_0(2\sqrt{\alpha\beta}) + 2\sqrt{\alpha\beta} I_1(2\sqrt{\alpha\beta}) \} \end{aligned} \quad \dots (4.15)$$

$$\begin{aligned} x_1(\alpha, \beta) &= R(x_{11} + x_{12}) \\ y_1(\alpha, \beta) &= R(y_{11} + y_{12}) \end{aligned} \quad \dots (4.16)$$

where $x_{11}, x_{12}, y_{11}, y_{12}$ are tabulated in Ref.7 for 5° intervals of α, β .

The further extension of the layout is illustrated in Fig.11. The curved lines A"D and the straight line A"C" determine a field of coordinate lines in the region A"C"D"D. These consist of straight lines and involutes of the type analysed in para.4.5. Exactly similar extensions can be found for B"EE"C", B'EE'C' and A'DD'C'. The pairs of lines C'D", C'E" and C'D', C'E' may now form the basis of further extension. For example coordinate lines may be drawn in the region C"D"HE" in much the same way as they were determined above beginning with the circles AA", AA' and developing a field in AA"DA'. Formulae and tables for the region C"D"HE" are also calculated in Ref.7. With displacements along α, β curves denoted by (u_2, v_2) , and Cartesian coordinates (x_2, y_2) tangential to the α, β curves at C", they are

$$\begin{cases} u_2(\alpha, \beta) = e_1 R(u_{21} + u_{22}) \\ v_2(\alpha, \beta) = \frac{e_2}{e_1} u_2(\beta, \alpha) \end{cases} \quad \dots (4.17)$$

$$\begin{cases} x_2(\alpha, \beta) = R(x_{21} + x_{22}) \\ y_2(\alpha, \beta) = R(y_{21} + y_{22}) \end{cases} \quad \dots (4.18)$$

and the functions $u_{21}, u_{22}, x_{21}, x_{22}, y_{21}, y_{22}$ are tabulated in Ref.7.

The next stage consists of filling the squares DD"FD', EE'GE' with orthogonal straight lines, followed by constructing layouts of straight lines and involutes in regions such as FJHD", GKHE".

Further developments should now be clear. In fact step by step construction in a similar manner to that described above will consistently determine a strain field with principal strain e_1 and e_2 extending over the whole plane.

Section 5. Conditions of Equilibrium

5.1 The principal stresses f_1 and f_2^* acting in a Michell plate will lie in the directions of coordinate lines α, β with layouts of the kind determined in Section 4. These stresses will be in equilibrium and using standard results given in for example Ref.6 art.331 the following equations are obtained for the case where body forces are absent.

$$\frac{\partial}{\partial \alpha}(Bt_p f_1) - At_p f_2 \frac{\partial \phi}{\partial \beta} = 0, \quad \frac{\partial}{\partial \beta}(At_p f_2) + Bt_p f_1 \frac{\partial \phi}{\partial \alpha} = 0$$

Here t_p is the plate thickness. These formulae can be expressed in a manner similar to that of (3.2) by introducing

$$T_1 = Bt_p f_1, \quad T_2 = At_p f_2 \quad \dots (5.1)$$

which must satisfy

$$\frac{\partial \phi}{\partial \alpha} = -\frac{1}{T_1} \frac{\partial T_2}{\partial \beta}, \quad \frac{\partial \phi}{\partial \beta} = \frac{1}{T_2} \frac{\partial T_1}{\partial \alpha} \quad \dots (5.2)$$

The determination of T_1 and T_2 is thus reduced to the same kind of problem as that presented by the calculation of A,B. [‡]

* The stars previously attached to these quantities in Section 2 will now be omitted.

‡ See Appendix B.

5.2 The integration of equations (5.2) requires the knowledge of suitable boundary conditions. These are determined by the conditions of equilibrium at the reinforcing members. Fig.12 shows the forces acting on elements of such members lying respectively along β and α lines.

The piece of the reinforcing member on the β -line has length $Bd\beta$ and carries a compressive end load P . External forces (F_α, F_β) per unit length are assumed to act and balance is achieved by a discontinuity in the plate stress resultant which is determined by T_1 . Equilibrium requires that

$$\Delta T_1 = -P \frac{\partial \phi}{\partial \beta} - F_\alpha B, \quad \frac{dP}{Bd\beta} = F_\beta \quad \dots (5.3)$$

and P follows from the second equation, when its value is known at an end of the reinforcing member.* The first equation then determines the discontinuity ΔT_1 in T_1 .

The second figure of Fig.12 shows an element of length $Ad\alpha$ carrying a tensile end load T . In this case equilibrium requires

$$\Delta T_2 = -T \frac{\partial \phi}{\partial \alpha} - F_\beta A, \quad \frac{dT}{Ad\alpha} = -F_\alpha \quad \dots (5.4)$$

and the boundary jump in T_2 is determined as before.

5.3 The values of plate thickness t_p , reinforcement area A_R and principal stresses f_1 and f_2 follow from the restrictions of (2.2) which are imposed upon the stresses of a Michell design. Taking as standard the cases where the virtual strain along the α -lines is $e_1 = +e$ or 0 and that along the β -lines is $e_2 = -e$ or 0 , equation (2.2) gives

$$f_1 - f_2 = f \quad \text{or} \quad f_1 = f \quad \text{or} \quad f_2 = -f$$

and so introducing T_1 and T_2 from (5.1), it follows that

* In the cases considered in this report pairs of reinforcing members begin at the points of action

$$t_p = \frac{1}{f} \left(\frac{T_1}{B} - \frac{T_2}{A} \right) \quad \text{or} \quad t_p = \frac{T_1}{Bf} \quad \text{or} \quad t_p = -\frac{T_2}{Af} \quad \dots (5.5)$$

in the three strain conditions considered. The values of f_1 and f_2 follow immediately if required.

The areas of the reinforcing members also follow from (2.2) they are

$$A_R = T/f \quad \text{or} \quad P/f \quad \dots (5.6)$$

as the case may be.

The plate thicknesses t_p and the areas of reinforcing members must of course satisfy

$$t_p \geq 0, \quad A_R \geq 0 \quad \dots (5.7)$$

in a proper Michell structure.

Section 6. First example of a Force Reacted at Two Fixed Supports. (Case when the Force is normal to the line of supports)

6.1 Let it be assumed that the two fixed points lie on a horizontal axis at distance d apart and let an origin be taken midway between the supports. The specified force F acts at a point $(l/d, h/d)$, where l is the horizontal distance from the origin and h is the height above the horizontal axis. Symmetry shows that it is necessary to consider only the first quadrant. In various regions of this quadrant, different layouts of structure are required, as indicated in Fig.13a.

6.2 Consider first the cases when F is acting on $l = 0$. The strain field Fig.7 is used with $e_1 = -e_2 = e$, and with the force F acting vertically at the origin O . The positions of points with zero horizontal displacement are then found. For $2\theta \operatorname{tg}\theta \geq 1$ ($\theta \geq 37^\circ 25'$), these points lie on the lines OC, OC'

with $OA/AC = (2\theta \operatorname{tg}\theta - 1)/(2\theta - \operatorname{tg}\theta) = OA'/A'C'$. The points C, C' can then be taken as the fixed supports and the structure then consists of a compression member CA A'C' joined to a plate AOA'. When $\theta = \pi/4$ the points C, O, C' are co-linear; this corresponds in Fig. 13a to the solution for F at the origin. When $\theta = 37^\circ 25'$, the points with zero horizontal displacements lie along OB_1 and OB'_1 in Fig. 7, so that the structure is reduced to a two bar frame. The height of point O above $B_1B'_1$ is given by the ratio $h/d \approx 0.38$.

If the force acts at a height $h \geq 0.38d$ above the supports, the structure is simply a two bar frame. This corresponds to the case $0 \leq \theta \leq 37^\circ 25'$ in Fig. 7. The points of zero horizontal displacement then lie in the hydrostatic fields OBB_1 and $OB'_1B'_1$. The angle subtended at O by the supports varies from $2 \times (90^\circ - 37^\circ 25') = 105^\circ 10'$ to zero, and the two bar frame gives the required solution for all $h \geq 0.38d$. More detailed analysis of this strain field is given in Appendix A.

6.3 Fig. 7 also gives solutions for $0 \leq l \leq \frac{d}{2}$ if the fan angle 2θ is replaced by $2\theta = \theta_1 + \theta_2$, where θ_1 is the angle between $B'OA$ and the vertical, θ_2 is the angle between $A'OB$ and the vertical. By varying the angles θ_1, θ_2 repeatedly from 0 to $\pi/4$, non-symmetrical structures of a similar form to those of the case $l = 0$ can be found. The only difficulty is that no structural layout results when $\theta_1 \geq 37^\circ 25'$ and $\theta_2 \leq 37^\circ 25'$, since this corresponds to the case when the points of zero horizontal displacement lie in $OACB_1$ and $OB'_1B'_1$ respectively. This small forbidden region is shown by the shaded area within $l \leq \frac{d}{2}$ in Fig. 13a.



6.4 The strain field of Figs.10, 11 can be used to obtain solutions for the case $l \geq \frac{d}{2}$. The points O and C are taken as the fixed supports. The point of action of the force F is restricted by the requirement that the applied force must put reinforcing members along the α -lines in tension and those along the β -lines in compression, so as to correspond with the strains $e_1 = -e_2 = e$. It follows that the force F must lie in the region $-\alpha + \beta = \phi \leq -\pi/4$ (see Fig.14). This is the lower right hand region of Fig.13a.

At the boundary of the region where $\alpha - \beta = \pi/4$, the force F is acting tangential to the bounding β -line of the structure. This suggests a modification to the strain field to give structures extending into the region above this boundary. Such a field is shown in Fig.15, where the tangent DD' to A'D at D is at right angles to OC. A'D is then used as a starting α -line which together with DD' generates a field of straight β -lines and involutes. The basic structure OA'DA'C together with the bar D'D will thus transfer the applied force from D to any point D' on DD' as indicated in Fig.13a.

6.4 Since the fan angle of Fig.10 cannot exceed $\frac{\pi}{2}$, solutions for the larger value of l/d must be sought from Fig.11. No structural layout results if the loading point lies in the region DA'BC'D". This is because the β -curves in this region by-pass the fixed points O and C. The shaded area in Fig.13a for $l \geq d/2$ indicates this further forbidden region.

If the force F is acting in the region D'CE'H, the resulting layout follows from Fig.11 and is shown in Fig.13a. As in the case treated in para.6.3, since members along α, β curves must carry stresses of opposite sign, only part of the region can be used. If C'E" and C'D" are taken as the starting α, β curves respectively, the region is restricted by $-\alpha + \beta \leq \pi/4$.

At the boundary $-\alpha+\beta = \pi/4$ and the applied force is tangential to the boundary β -curves. When the force is applied above this boundary, the optimum structure will consist of the basic structure on the boundary together with an additional strut (see Fig.13a).

6.5 Although there still remains limited regions of the quadrant where the optimum is unknown, it is possible interpolating from the existing knowledge, to calculate and plot lines of constant structural volume over the whole of the quadrant. Equation (1.6) may be used to calculate the volume of the optimum structures. This requires the knowledge of the virtual displacements of the corresponding strain fields. As already mentioned in section 4, the required information has been tabulated in Ref.7. The results of the appropriate calculations are shown in Fig.13b, where lines of constant volume are plotted using a non-dimensional parameter.

Section 7. Second Example of a Force Reacted at Two Fixed Points. (Case when the Force is Parallel to the line of supports)

7.1 The two fixed points are assumed to lie on a vertical axis at a distance d apart. An origin is taken midway between the supports. By symmetry, only the cases where the force is acting in a quadrant need to be considered. Any point in this quadrant will be specified by the coordinates $(l/d, h/d)$ which are defined in Fig.16a. For different regions in the quadrant different structural layouts are required (See Fig.16a).

- 7.2 When the force F is acting on $l = 0$, so that the point of action is collinear with the supports, the structure is simply a strut joining the point of action to the nearest support.
- 7.3 For a small region near the origin with $l \leq d/2$, the structures are found to be two bar frames. The strain field of Fig.6 is the basis of this conclusion. The origin O in Fig.6 is taken as the point of action of the force. For an arbitrary point D in $A'OA$, the locus of points D' in $B'OB$ is found for which the distance $D'D$ remains unchanged after the virtual deformation. Since the members OD and OD' will have strains of opposite sign, they correspond to a two bar frame carrying forces from O to D and D' , which can be regarded as fixed supports. Such structures cover the region indicated in Fig.6. At the point $l = d/2$, $h = 0$, the structure consists of the two members OA , OB of Fig.6, which is the limiting structure derivable from Fig.6.
- 7.4 For the case $l \geq d/2$, the strain field on Fig.10 is used. The applied force is now parallel to the fixed line OC . In order that the stresses correspond to the strain system $e_1 = -e_2 = e$, it is necessary to restrict attention to that part of region $A'DA$ for which $-\alpha + \beta = \phi \leq \pi/4$. At the boundary $-\alpha + \beta = \pi/4$, the force F is acting tangential to the bounding β -line of the structure. For the region beyond this boundary, the force may be transmitted by a strut to the basic structure at the boundary (see Fig.16a).
- 7.5 With the knowledge of the optimum structures for most of the quadrant (except for the shaded region), it is possible with a little interpolation to plot lines of constant volume. The result is shown in Fig.16b using a non-dimensional parameter $V^* = Vf/Fd$.

Section 8. Examples of the Determination of Volumes, Plate Thicknesses and Reinforcing Member Sizes

Ex. 8.1 Three parallel forces.

Consider the case of a force F acting normal to the line of two supports with $l = 3.2342d$, $h = 0$. From the results of Fig.13a, the optimum structure is found by using Fig.11 with the force acting in the region C "D" HE". Some details of the layout are shown in Fig.17. The fan angles of the structure are exactly $\alpha = \beta = 20^\circ = \mu$ in this case. (If the dimensions of the structure do not coincide with a multiple of 5° of the fan angles, interpolation using (4.18) is necessary to find the boundary α, β values).

Volume of the structure

Since F is acting at a point $\alpha = \beta$, the angle $\phi = -\alpha + \beta$ between the α -curve and the x_2 -axis at the point of action is zero. Resolving the virtual displacements in the direction of the force, the virtual work done is then, from (4.17) with

$$e_1 = -e_2 = e$$

$$\begin{aligned} W &= F(u_2 \cos \pi/4 - v_2 \sin \pi/4)_{\alpha=\beta=\mu} \\ &= \sqrt{2} eRF(u_{21} + u_{22})_{\alpha=\beta=\mu} \end{aligned}$$

From Eq.(1.6), the volume of the structure is, using the tables in Ref.7,

$$\begin{aligned} V_m &= \frac{W}{fe} = \frac{\sqrt{2}RF}{f}(u_{21} + u_{22})_{\alpha=\beta=\mu} \\ &= \frac{dF}{f}(u_{21} + u_{22})_{\alpha=\beta=\mu} = 15.3953 \frac{dF}{f} \end{aligned}$$

Reinforcing members

To transmit the concentrated force F it is clear, first of all that two reinforcing members are required along $OA'DD''P$ and $OB'EE''P$ to carry direct loads $\pm F/\sqrt{2}$. The area of these members will be $A_R = F/\sqrt{2}f$.

Thickness of the plate

The thickness of the plate must be worked out in successive regions starting from $C'D''PE''$. By symmetry, only half of the structure needs to be determined.

(a) In the regions $C'D''PE''$ ($0 \leq \alpha \leq \mu, 0 \leq \beta \leq \mu$).

The boundary conditions for T_1, T_2 follow from (5.3), (5.4), since $\phi = -\alpha + \beta, F_\alpha = F_\beta = 0$ and $T = P = F/\sqrt{2}$, as:

$$\begin{aligned} \text{on } D''P (\beta = \mu) : \quad T_2(\alpha, \mu) &= -\Delta T_2 = -F/\sqrt{2} \\ \text{on } E''P (\alpha = \mu) : \quad T_1(\mu, \beta) &= -\Delta T_1 = F/\sqrt{2} \dots \end{aligned} \quad (8.1)$$

Solving Eq.(5.2) with boundary conditions (8.1), the results are (see Appendix B),

$$T_1(\alpha, \beta) = \frac{F}{\sqrt{2}} \left\{ I_0(2\sqrt{(\mu-\alpha)(\mu-\beta)}) + \sqrt{\frac{\mu-\alpha}{\mu-\beta}} I_1(2\sqrt{(\mu-\alpha)(\mu-\beta)}) \right\} \dots \quad (8.2)$$

$$T_2(\alpha, \beta) = -T_1(\beta, \alpha)$$

The metric functions A and B in this region are known (from Eq.(21), Ref.7) as

$$\begin{aligned} A(\alpha, \beta) = R \left\{ I_0(2\sqrt{\alpha(\beta+\frac{\pi}{2})}) + I_0(2\sqrt{\beta(\alpha+\frac{\pi}{2})}) + \sqrt{\frac{\beta}{\alpha+\frac{\pi}{2}}} I_1(2\sqrt{\beta(\alpha+\frac{\pi}{2})}) \right. \\ \left. + \sqrt{\frac{\beta+\frac{\pi}{2}}{\alpha}} I_1(2\sqrt{\alpha(\beta+\frac{\pi}{2})}) \right\} \dots \end{aligned} \quad (8.3)$$

$$B(\alpha, \beta) = A(\beta, \alpha) .$$

Following Eq.(5.5), the plate thickness in the region is

$$t_p = \frac{1}{f} \left(\frac{T_1}{B} - \frac{T_2}{A} \right),$$

where the functions on the right-hand side are given by (8.2) and (8.3). Numerical values of the Bessel functions can be found in Ref.7 for α, β as multiples of 5° .

As an example, the thickness of the plate at the loading point P is calculated as follows:

$$\begin{aligned} T_1(\mu, \mu) &= -T_2(\mu, \mu) = F/\sqrt{2} \\ A(\mu, \mu) &= B(\mu, \mu) = 6.7013R \end{aligned}$$

$$\therefore t_p = \frac{2}{6.7013} \frac{F}{\sqrt{2Rf}} = 0.2984 \frac{F}{\sqrt{2Rf}} = 0.2984 \frac{F}{df}$$

(b) In the region DA "C"D" ($0 \leq \alpha \leq R$,^{*} $0 \leq \beta \leq \mu$)

The origin of the coordinate (α, β) is taken at A". α -curves are straight lines, so that T_1 does not change along an α -line from the boundary C"D" to A"D. From (8.2), the value of T_1 on C"D" ($\alpha = R$) is

$$T_1(R, \beta) = \frac{F}{\sqrt{2}} \left[I_0(2\sqrt{\mu(\mu-\beta)}) + \sqrt{\frac{\mu}{\mu-\beta}} I_1(2\sqrt{\mu(\mu-\beta)}) \right] \dots (8.4)$$

The metric function B in this region is, from (4.7)

$$B(\alpha, \beta) = \alpha + F(\beta) = \alpha + B(0, \beta)$$

where $B(0, \beta)$ is the value of B at A"D ($\alpha = 0$).

Equation (4.14), with $\alpha = \pi/2$, gives

$$B(0, \beta) = R \left[I_0(\sqrt{2\pi\beta}) + \sqrt{\frac{\pi}{2\beta}} I_1(\sqrt{2\pi\beta}) \right] \dots (8.5)$$

^{*} In this region α is the distance along the normals to A"D (cf. para.4.5)

The thickness distribution of the plate is then given by

$$t_p = \frac{T_1}{Bf} = \frac{T_1(R, \beta)}{Bf} .$$

(c) In the region A'AA''D ($0 \leq \alpha \leq \pi/2$, $0 \leq \beta \leq \mu$) .

The origin of the curvilinear coordinates in this region is taken at A. Boundary values of T_1 , T_2 are given by (8.1) and (8.4):

$$\text{on A'D } (\beta = \mu): \quad T_2(\alpha, \mu) = -F/\sqrt{2}$$

$$\text{on A''D } (\alpha = \pi/2): \quad T_1(\frac{\pi}{2}, \mu) = \frac{F}{\sqrt{2}} \left[I_0(2\sqrt{\mu(\mu-\beta)}) + \sqrt{\frac{\mu}{\mu-\beta}} I_1(2\sqrt{\mu(\mu-\beta)}) \right] .$$

Solving Eqs.(5.2) with the above boundary conditions and $\phi = -\alpha + \beta$, gives the results :

$$T_1(\alpha, \beta) = \frac{F}{\sqrt{2}} \left[I_0(2\sqrt{(\frac{\pi}{2}+\mu-\alpha)(\mu-\beta)}) + \sqrt{\frac{\pi+\mu-\alpha}{\mu-\beta}} I_1(2\sqrt{(\frac{\pi}{2}+\mu-\alpha)(\mu-\beta)}) \right]$$

$$T_2(\alpha, \beta) = \frac{-F}{\sqrt{2}} \left[I_0(2\sqrt{(\frac{\pi}{2}+\mu-\alpha)(\mu-\beta)}) + \sqrt{\frac{\mu-\beta}{\pi+\mu-\alpha}} I_1(2\sqrt{(\frac{\pi}{2}+\mu-\alpha)(\mu-\beta)}) \right] . \quad \dots (8.6)$$

and the plate thickness is $t_p = \frac{1}{f} \left(\frac{T_1}{B} - \frac{T_2}{A} \right)$, where A, B are given by (4.14).

(d) In the region ACA'', A'OA

T_2 (T_1) remains unchanged from the boundary AA'' (A'A) to the singular point C(0). The values of T_2 , T_1 on the boundaries are given by (8.6): $T_2 = T_2(\alpha, 0)$, $T_1 = T_1(0, \beta)$. The thickness of the plate in these regions is

$t_p = -\frac{T_2(\alpha, 0)}{rf}$ or $\frac{T_1(0, \beta)}{rf}$, where r is the distance from the singular point C or O.

Diagram of thickness distribution

The procedure for obtaining a diagram of contours of constant thicknesses, Fig.18, is as follows,

(a) In general the thicknesses of the plate at the points where α, β is a multiple of 5° are calculated by using the tables of Ref.7. In the case where the α -curves are straight lines, the thicknesses can be determined at chosen positions on the α -lines. See Fig.19.

(b) The positions of points (α, β) with reference to a cartesian coordinate system are determined by using Eqs.(4.16), (4.18). For example, the relation between the coordinates $x = \frac{1}{2}(x_2+y_2)$ in the region C'D'PE" and $l = \frac{1}{2}(x_1-y_1)\frac{d}{R}$ in the region A'AA"D and the α, β coordinates is shown in Fig.20.

(c) Values of constant thickness are then interpolated at points on an α -curve or a β -curve using (a), and the corresponding positions in space are obtained from (b).

(d) Contours of constant thickness are then plotted, introducing the non-dimensional variable $t_p \frac{df}{F}$ (Fig.18).

(e) The reinforcing members can be determined so that they are of the same thickness as the plate on the contour line $t_p \frac{df}{F} = 8$. Since

$$A_R = \frac{F}{\sqrt{2}f} = \frac{F}{\sqrt{2}fR} \cdot R = \frac{F}{df} \cdot R \text{ or } A_R \cdot \frac{df}{F} = R,$$

the width of the reinforcing member is $R/8$.

When the magnitude of the force F is given, the design will be completely determined by the value of the parameter df/F .

Ex. 8.2 Symmetrical Cantilever.

The volume and thickness distribution of a 60° cantilever shown in Fig.21 is determined in this example.

Volume of the structure

The α , β curves intersect the line of symmetry AP at 45° , and so the force F bisects the α , β directions at P. Using (4.15) with $e_1 = -e_2 = e$, $\alpha = \beta = 60^\circ = \mu$, the volume of the structure is obtained from (1.6):

$$\begin{aligned} V_m &= \frac{W}{fe} = \frac{F}{fe} (u_1 \cos \frac{\pi}{4} - v_1 \sin \frac{\pi}{4})_{\alpha=\beta=\mu} \\ &= \frac{\sqrt{2FR}}{f} \left[(1+2\mu)I_0(2\mu) + 2\mu I_1(2\mu) \right] \\ &= 11.1764 \frac{Fd}{f} . \end{aligned}$$

Reinforcing members

The boundary α , β curves are OA'P and CA''P respectively. Members along these lines must carry direct loads $\frac{F}{\sqrt{2}}$ from P to the supports O and C. The area of the reinforcing members is $A_R = \frac{F}{\sqrt{2}f}$.

Thickness of the plate

(a) In region AA'PA''

This region is bounded by AA'' ($\beta = 0$), AA' ($\alpha = 0$), A'P ($\beta = \mu$) and A''P ($\alpha = \mu$). Using Eqs. (5.3), (5.4), the boundary values of T_1 , T_2 are

$$\begin{aligned} \text{on A'P : } T_2(\alpha, \mu) &= -\Delta T_2 = -F/\sqrt{2} \\ \text{on A''P : } T_1(\mu, \beta) &= -\Delta T_1 = F/\sqrt{2} \end{aligned}$$

Solving Eq.(5.2) with the above boundary conditions gives, as in (8.2),

$$T_1(\alpha, \beta) = \frac{F}{\sqrt{2}} \left[I_0(2\sqrt{(\mu-\alpha)(\mu-\beta)}) + \sqrt{\frac{\mu-\alpha}{\mu-\beta}} I_1(2\sqrt{(\mu-\alpha)(\mu-\beta)}) \right] \dots (8.7)$$

$$T_2(\alpha, \beta) = -T_1(\beta, \alpha)$$

so that the plate thickness is $t_p = \frac{1}{f} \left(\frac{T_1}{B} - \frac{T_2}{A} \right)$ where A, B are given by (4.14).

(b) In region OA'A and CAA''.

Since one set of coordinate curves are straight lines, T_1 (T_2) does not change from the boundary AA' (AA'') to the singular point O(C). The plate thickness is $t_p = \frac{T_1(0, \beta)}{rf}$ or $\frac{-T_2(\alpha, 0)}{rf}$, where $T_1(0, \beta)$, $T_2(\alpha, 0)$ are given by (8.7) and r is the distance from the singular point O or C.

Diagram of thickness distribution (Fig.22)

The quantities in (8.7) and (4.14) can be calculated for 5° intervals of α, β by using the tables in Ref.7. The thickness distribution is then obtained as follows:

(a) The thicknesses of the plate at the points where α, β is a multiple of 5° are calculated and plotted in Fig.23.

(b) The positions of these points referred to a Cartesian coordinate system are determined by using Eq.(4.16). In the region A'AA''P taking coordinates $x = \frac{1}{2}(x_1 + y_1) \frac{d}{R}$ at A, the result is shown in Fig.24.

(c) In the regions OA'A and CAA'', the thickness along a radius is inversely proportional to the distance from the singular point.

(d) Values of constant thicknesses are then interpolated along the α, β curves using the result of (a) and (b).

(e) Contours of constant thicknesses are plotted for the non-dimensional value $t_p \frac{df}{F}$ in Fig.22.

(f) The reinforcing members are determined so that they are of the same thickness as the plate at the contour line $t_p \frac{df}{F} = 8$. Since $A_R \frac{df}{F} = R$, the width of the reinforcing members is $R/8$, as shown in Fig.22.

Reacting forces at the supports

The reactions at O and C can, in this case, be determined from statics. In general, it is required to integrate the forces in the plate acting at O or C. For example, the forces in the region OA'A are known to be $T_1(0, \beta)$. The vertical and horizontal components of the resultant at O are thus

$$-\frac{F}{2} = \frac{F}{\sqrt{2}} \sin(\mu - \frac{\pi}{4}) + \int_0^{\mu} T_1(0, \beta) \sin(\beta - \frac{\pi}{4}) d\beta ,$$

and

$$F \cdot \frac{l}{d} = \frac{F}{\sqrt{2}} \cos(\mu - \frac{\pi}{4}) + \int_0^{\mu} T_1(0, \beta) \cos(\beta - \frac{\pi}{4}) d\beta ,$$

which can be verified with the aid of the integration formulae given in Ref.7.

Section 9. Method of Approximate Numerical Analysis

9.1 The exact solutions of Michell structures as demonstrated in the previous sections require the knowledge of the deformation fields. Only few such fields are at present known and lack of knowledge is especially marked in three-dimensions. Methods of approximate determination of minimum weight structure are thus of great interest. For pin-jointed Michell frames, good approximation can be achieved by using the method of linear programming, (see for instance Ref.8).

9.2 In the general formulation of para.1.2, imagine the region to be covered by a grid of points P, which includes the points of application of F and the points where structural joints are to be located. Generally in three-dimensional space, each point P_i is specified by three coordinates (x_1^i, x_2^i, x_3^i) and these are three components of force (F_1^i, F_2^i, F_3^i) and virtual displacement (u_1^i, u_2^i, u_3^i) at each point. Possible structural members are assumed to lie along the segments joining any pair of the points, P_i and P_j say, for which (1.2) must be satisfied; i.e. for any i, j

$$\left| \sum_{k=1}^3 (x_k^i - x_k^j)(u_k^i - u_k^j) \right| \leq e \sum_{k=1}^3 (x_k^i - x_k^j)^2 \quad \dots (9.1)$$

The work done is then expressed by,

$$W = \sum_j \sum_{k=1}^3 F_k^j u_k^j, \quad \dots (9.2)$$

where j is summed over all points P. Labelling the forces and displacements for all points in sequence, from 1 to n say, the optimisation problem can be formulated from (1.6) as:

$$\text{To find } fV_m = \max. \sum_{i=1}^n F_i v_i \quad \dots (9.3)$$

$$\text{subject to } \left| \sum_{i=1}^n a_{ij} v_i \right| \leq l_j, \quad j = 1 \dots m, \quad \dots (9.4)$$

where ev_i is a typical virtual displacement, and the coefficients a_{ij} , l_j , F_i are determined by the geometry and the applied forces according to (9.1) and (9.2). The numbers n, m specify the size of the problem. On a grid of k points in space, the greatest possible values of n and m are $n = 3k$, $m = C_2^k$.

9.3 The problem (9.3)-(9.4) can be solved by the methods of linear-programming, for example, using the simplex method (Ref.8, Ch.3). However it differs from the standard formulation in two aspects. Firstly, Eqs. (9.4) involve absolute-values, which can be rewritten as

$$\begin{aligned} \sum_{i=1}^n a_{ij}v_i + y_j &= l_j, \\ 0 \leq y_j &\leq 2l_j, \end{aligned} \quad j = 1, \dots, m \dots (9.5)$$

The variables y_j are not allowed to exceed $2l_j$ (the so-called upper bound condition). In actual computation, only the first line of (9.5) need to be stored, (see Ref.8, p.387).

Secondly, the variables v_i can be positive or negative, which is not usually taken into account by the standard computing programmes. However, the simplex method can be modified to deal with this situation, (see Ref.9).

A computing programme based on the simplex method with these modifications has been written on the Pegasus computer. Two examples of the results of computing will be given below. An example in three-dimensional space can be found in Ref.10.

Ex. 9.1 The loading system is shown in Fig.25a with $l = 3d$. The virtual deformation is assumed to be antisymmetrical about OD and the grid used for its analysis is shown in Fig.25b. There are 33 variables and 125 inequalities of the form (9.4). This figure also shows the value of v which maximise the work done by the force F . The layout of potential structural members, made up of those segments which have strains $\pm e$ (i.e. the corresponding constraints (9.4) are satisfied as Eqs.) is shown in Fig.25c and a structure formed from them is given in Fig.25d.*

*This is a special case. The most general structure formed from Fig.12 is three-fold redundant. Its volume is of course independent of the redundancies.

The structure of Fig.25d is the optimum on the grid and has a volume $v_m = 13.83 Fd/f$. Compared with the exact solution to the problem given in Fig.16a, the above approximation is only some 6 per cent above the ideal value.

Ex.9.2. The loading system is shown in Fig.26a where C,C' are fixed supports. A grid with the value of v which maximise the work done by the force F is shown in Fig.26b. There are 26 variables and 73 inequalities of the form (9.4) involved in the analysis. The layout of potential structural members is shown in Fig.26c and the only structure formed from them is given in Fig.26d. The volume of the structure, as indicated by the value v at P, is $v_m = 9 Fd/f$. The structure resulting from this computation led directly to the discovery of the strain field of Fig.15.

Section 10. Future Developments

The subject has now reached the stage where data for practical application can be produced. A data sheet for a force parallel to two fixed supports or indeed at any angle could now be drawn with very little further work. Extension to the more general case of three specified forces in equilibrium, which is under consideration at the moment, will doubtless be resolved by further research. A series of appropriate layouts are known which depend upon a variable parameters, which by adjustment will permit a measure of control on the nature of the reacting forces. The resolution of the three force problem now seems a realisable objective for future research.

The general two-dimensional problem for any layout of given forces and supports and for a variety of loading cases, can of course be solved by the numerical methods. However as things stand at the moment the calculations are rather large in extent and further research to develop more powerful techniques is necessary. This should results, in the long run, in standard

programmes for the approximate determination of the best reinforced plate or framework structures for two-dimensional problems.

The extension of this work to space structures, in particular to reinforced shells, is at present in its infancy. The active pursuit of this problem is of great engineering interest and should constitute a long term aim of the research programme.

References

1. Michell, A.G.M. The Limit of Economy of Material in Frame Structures.
Phil.Mag.S.6.,Vol.8,No.47, London,Nov. 1904.
2. Hill, R. The Mathematical Theory of Plasticity.
Clarendon Press, Oxford, 1950.
3. Prager, W. On a Problem of Optimum Design.
Brown Univ.Div. of App. Maths. Tech.Report 38,
1958.
4. Hemp, W.S. Theory of Structural Design.
College of Aero. Report 115, 1958.
5. Chan, A.S.L. The Design of Michell Optimum Structures.
College of Aero. Report 142, 1960.
6. Love, A.E.H. A Treatise on the Mathematical Theory of
Elasticity, 4th Edition, Cambridge Univ.
Press, 1927.
7. Chan, H.S.Y. Tabulation of some layouts and virtual
displacement fields in the theory of Michell
optimum structures.
College of Aeronautics, Note Aero.161, 1964.
8. Hadley, G. Linear Programming.
Addison-Wesley 1962.
9. Dorn, W.S. Linear Programming and plastic limit analysis
Greenberg, H.J. of structures.
Quart. Appl. Maths., V.15,1957.
10. Chan, H.S.Y. Optimum structural design and linear
programming.
College of Aeronautics Report Aero.175, 1964.

Appendix A

Detailed Analysis of Fig.7.

Fig.7 is reproduced as Fig.27 in order to show to various coordinate systems which it is convenient to introduce. (α_1, β_1) is a system of polar coordinates to be used in OAA'. (α_2, β_2) are Cartesian coordinates for the region OA'C'B₁' , which are also used in OB₁'B₁' . (α_3, β_3) are polar coordinates in OBB' . Finally (x, y) are Cartesian coordinates with Oy along the line of symmetry of the figure.

Attention will be directed to the special case, required for application, for which

$$e_1 = e, \quad e_2 = -e \quad \dots (A.1.)$$

Also for simplicity O will be taken as a fixed point and Oy as a line of zero transverse displacement.

Equation (4.6) gives for the region OAA'

$$u_1 = e\alpha_1, \quad v_1 = -2e\alpha_1\beta_1 \quad \dots (A.2.)$$

This determines the displacements on OA' and so by (4.2) gives

$$u_2 = e\alpha_2 + 2e\theta\beta_2, \quad v_2 = -e\beta_2 - 2e\theta\alpha_2 \quad \dots (A.3.)$$

for the region OA'C'B₁' . Equation (4.2) may also be used to find the displacements in OB₁'B₁' , by writing $e_1 = e_2 = -e$ and matching displacements along $\alpha_2 = 0$ with those of (A.3).

This gives

$$u_2 = -e\alpha_2 + 2e\theta\beta_2, \quad v_2 = -e\beta_2 - 2e\theta\alpha_2 \quad \dots (A.4)$$

The relation between the coordinates (α_2, β_2) and (α_3, β_3) at the line OB' is

$$\alpha_2 = -\beta_3 \cos 2\theta, \quad \beta_2 = \beta_3 \sin 2\theta$$

and that between the corresponding displacement components on this same line is

$$u_3 = u_2 \sin 2\theta + v_2 \cos 2\theta, \quad v_3 = -u_2 \cos 2\theta + v_2 \sin 2\theta$$

Using (A.4) gives for the line OB' the result

$$u_3 = 2e\theta\beta_3, \quad v_3 = -e\beta_3,$$

which agrees with the displacements in OBB' , which after the manner of (A.2) may be shown to be

$$u_3 = 2e\alpha_3\beta_3, \quad v_3 = -e\beta_3 \quad \dots (A.5.)$$

Application of this strain field requires a knowledge of those points for which the displacement u_x parallel to Ox is zero. In the region $OA'C'B'_1$

$$u_x = -u_2 \sin \theta - v_2 \cos \theta$$

and so by (A.3) $u_x = 0$ occurs on the line with slope

$$\beta_2/\alpha_2 = \frac{(2\theta \cos \theta - \sin \theta)}{(2\theta \sin \theta - \cos \theta)} \quad \dots (A.6.)$$

When $\theta = \pi/4$, $\beta_2/\alpha_2 = 1$ and, as is clear from Fig.6, the locus of points with $u_x = 0$ consists of the line $C'OC$, which in this case coincides with Ox . As θ decreases the line of zero u_x turns towards OB'_1 and coincides with it when $\cot \theta = 2\theta$ or $\theta \simeq 37^\circ 25'$.

In the region $B'OB'_1$ the locus given by $u_x = 0$ has after (A.4) the equation

$$\beta_2/\alpha_2 = \frac{2\theta \cos\theta + \sin\theta}{2\theta \sin\theta - \cos\theta} \quad \dots (A.7.)$$

This is a line in $B'OB'_1$ so long as $-\infty \leq \beta_2/\alpha_2 \leq -\tan 2\theta$. The lower limit gives $\cot\theta \geq 2\theta$ or $\theta \leq 37^\circ 25'$, whereas the upper limit imposes no restriction.

Appendix B

Analytical Method For Integrating the
Hyperbolic Differential Equations

For the deformation fields considered in Figs.10 and 11,
 $\phi = -\alpha + \beta$. Eqs.(3.2), (5.2) and the first two of (3.4) then
become

$$\frac{\partial A}{\partial \beta} = B, \quad \frac{\partial B}{\partial \alpha} = A; \quad \dots (B.1)$$

$$\frac{\partial T_2}{\partial \beta} = T_1, \quad \frac{\partial T_1}{\partial \alpha} = T_2; \quad \dots (B.2)$$

and
$$\frac{\partial u}{\partial \alpha} + v = e_1 A, \quad \frac{\partial v}{\partial \beta} + u = e_2 B. \quad \dots (B.3)$$

Equations (B.1), (B.2) give immediately

$$\begin{aligned} \frac{\partial^2 A}{\partial \alpha \partial \beta} - A &= 0, & \frac{\partial^2 B}{\partial \alpha \partial \beta} - B &= 0, \\ \frac{\partial^2 T_1}{\partial \alpha \partial \beta} - T_1 &= 0, & \frac{\partial^2 T_2}{\partial \alpha \partial \beta} - T_2 &= 0, \end{aligned} \quad \dots (B.4)$$

while (B.3) gives, by using (B.1):

$$\begin{aligned} \frac{\partial^2 u}{\partial \alpha \partial \beta} - u &= (e_1 - e_2)B, \\ \frac{\partial^2 v}{\partial \alpha \partial \beta} - v &= -(e_1 - e_2)A. \end{aligned} \quad \dots (B.5)$$

The equations (B.4), (B.5) are hyperbolic differential equations of the form

$$\frac{\partial^2 H}{\partial \alpha \partial \beta} - H = G, \quad \dots (B.6)$$

where G is a known function of α, β .

Given boundary values $H(\alpha, 0), H(0, \beta)$, Eq.(B.6) can be solved by means of Riemann's method, which gives

$$\begin{aligned} H(\alpha, \beta) = & H(0, 0) I_0(2\sqrt{\alpha\beta}) + \int_0^\alpha I_0(2\sqrt{(\alpha-\xi)\beta}) \frac{\partial H(\xi, 0)}{\partial \xi} d\xi \\ & + \int_0^\beta I_0(2\sqrt{\alpha(\beta-\eta)}) \frac{\partial H(0, \eta)}{\partial \eta} d\eta \\ & + \int_0^\alpha \int_0^\beta I_0(2\sqrt{(\alpha-\xi)(\beta-\eta)}) G(\xi, \eta) d\xi d\eta \quad \dots (B.7) \end{aligned}$$

The success of this method depends on whether the integrations in (B.7) can be performed readily. Some analytical results for this kind of integral are given in Ref.7, and are sufficient to obtain solutions for the present purpose.

As an example, assume the boundary values are given on the lines $\alpha = \mu, \beta = \mu$ and that it is required to find $T_1(\alpha, \beta), T_2(\alpha, \beta)$ for $0 \leq \alpha \leq \mu, 0 \leq \beta \leq \mu$. Let

$$T_1(\mu, \beta) = C_1 \quad \text{on } \alpha = \mu,$$

$$T_2(\alpha, \mu) = C_2 \quad \text{on } \beta = \mu,$$

where C_1, C_2 are constants. A transformation is needed in order to apply (B.7). Setting $\alpha = \mu - \xi, \beta = \mu - \eta$ the boundary values become

$$T_1(\mu, \mu - \eta) = C_1 \quad \text{on } \xi = 0,$$

$$T_2(\mu - \xi, \mu) = C_2 \quad \text{on } \eta = 0,$$

and it is required to obtain values of $T_1(\mu-\xi, \mu-\eta)$, $T_2(\mu-\xi, \mu-\eta)$ for $0 \leq \xi \leq \mu$, $0 \leq \eta \leq \mu$. Eq.(B.7) gives, by using (B.2) and writing $H(\xi, \eta) = T_1(\mu-\xi, \mu-\eta)$

$$\begin{aligned} T_1(\mu-\xi, \mu-\eta) &= H(\xi, \eta) = T_1(\mu, \mu) I_0(2\sqrt{\xi\eta}) - \int_0^\xi I_0(2\sqrt{(\xi-t)\eta}) T_2(\mu-t, \mu) dt \\ &= C_1 I_0(2\sqrt{\xi\eta}) - C_2 \int_0^\xi I_0(2\sqrt{(\xi-t)\eta}) dt \\ &= C_1 I_0(2\sqrt{\xi\eta}) - C_2 \sqrt{\frac{\xi}{\eta}} I_1(2\sqrt{\xi\eta}) . \end{aligned}$$

i.e. $T_1(\alpha, \beta) = C_1 I_0(2\sqrt{(\mu-\alpha)(\mu-\beta)}) - C_2 \sqrt{\frac{\mu-\alpha}{\mu-\beta}} I_1(2\sqrt{(\mu-\alpha)(\mu-\beta)}) .$

Similarly

$$T_2(\alpha, \beta) = C_2 I_0(2\sqrt{(\mu-\alpha)(\mu-\beta)}) - C_1 \sqrt{\frac{\mu-\beta}{\mu-\alpha}} I_1(2\sqrt{(\mu-\alpha)(\mu-\beta)}) .$$

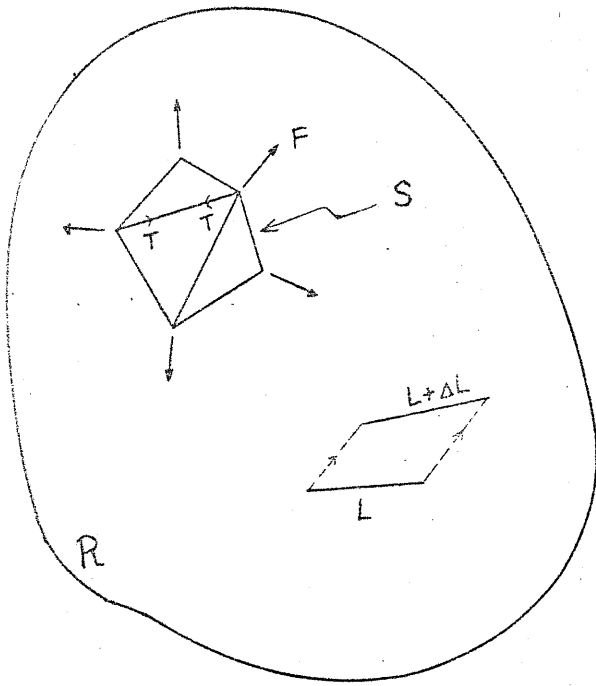


FIG. 1

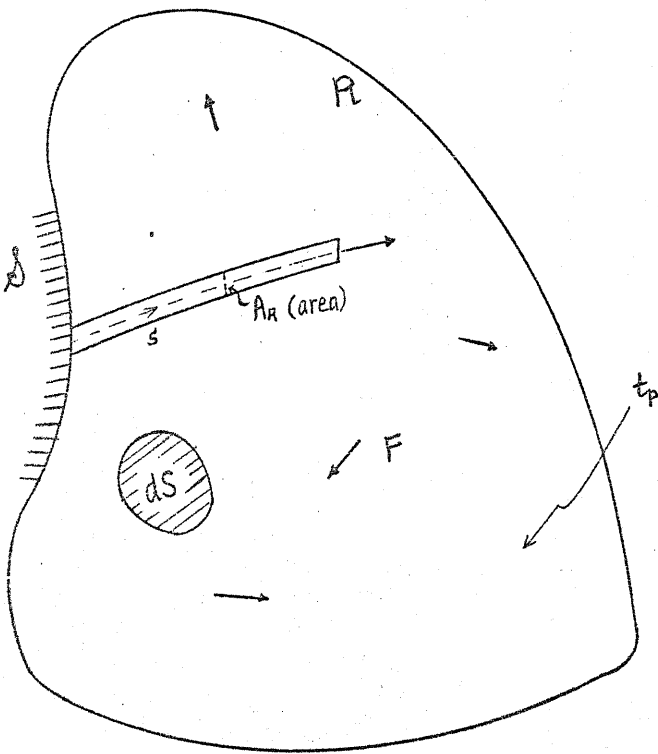


FIG. 2

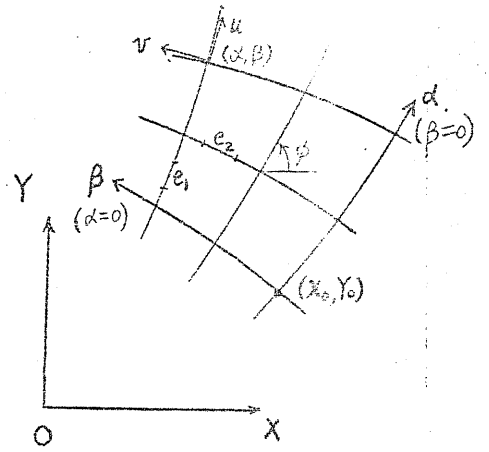


FIG. 3

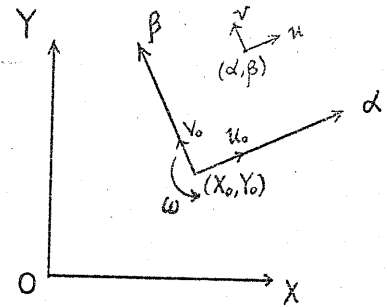


FIG. 4

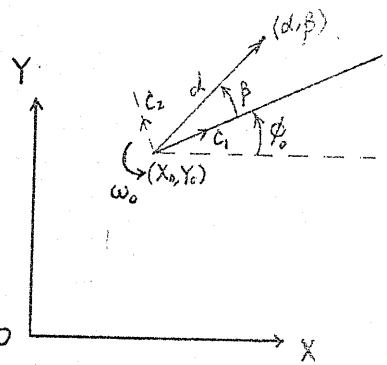


FIG. 5

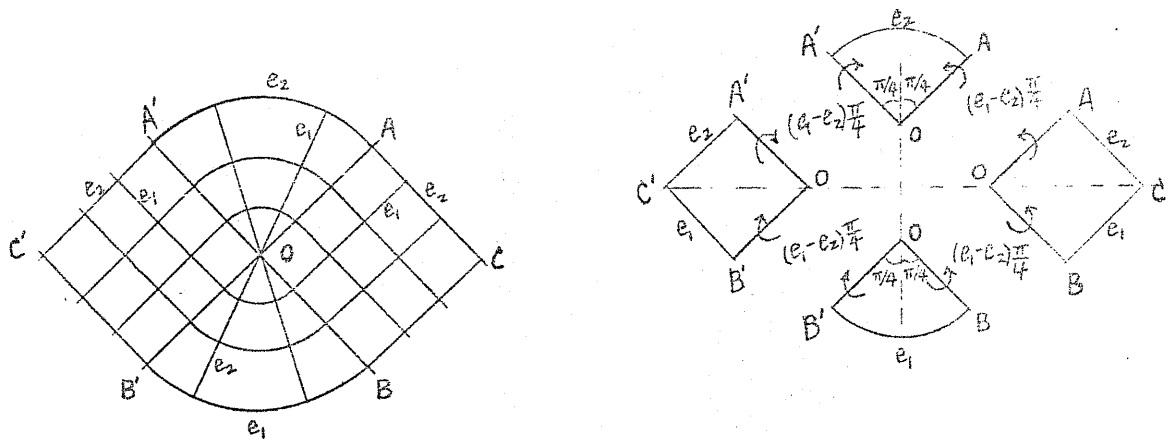


FIG. 6

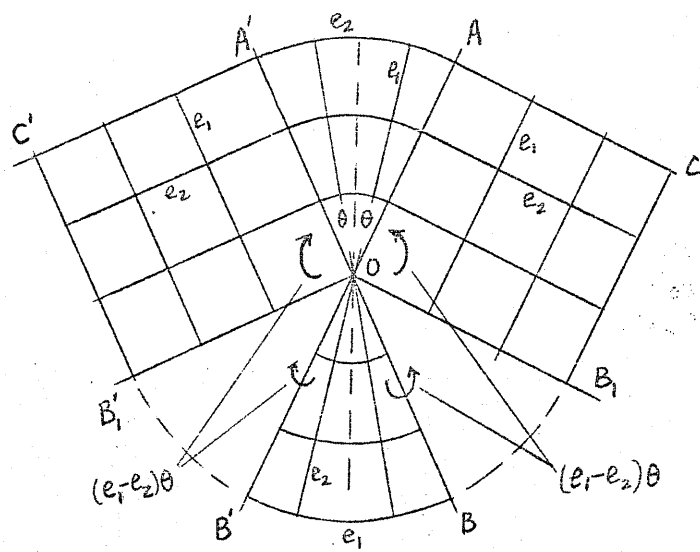


FIG. 7

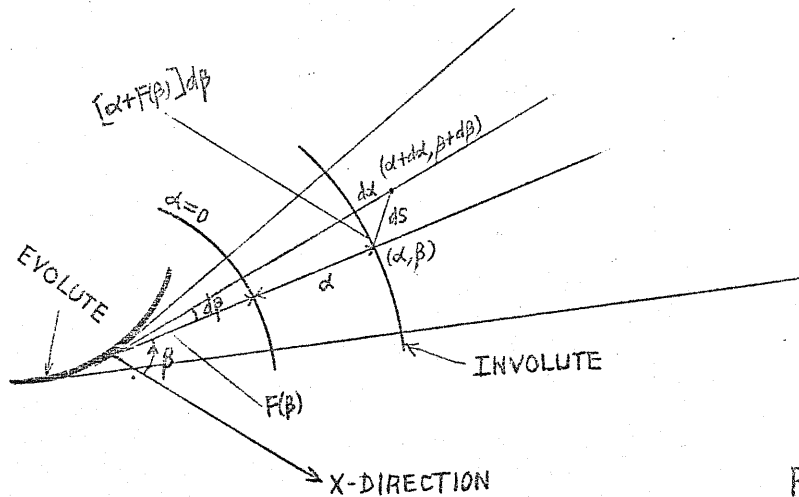


FIG. 8

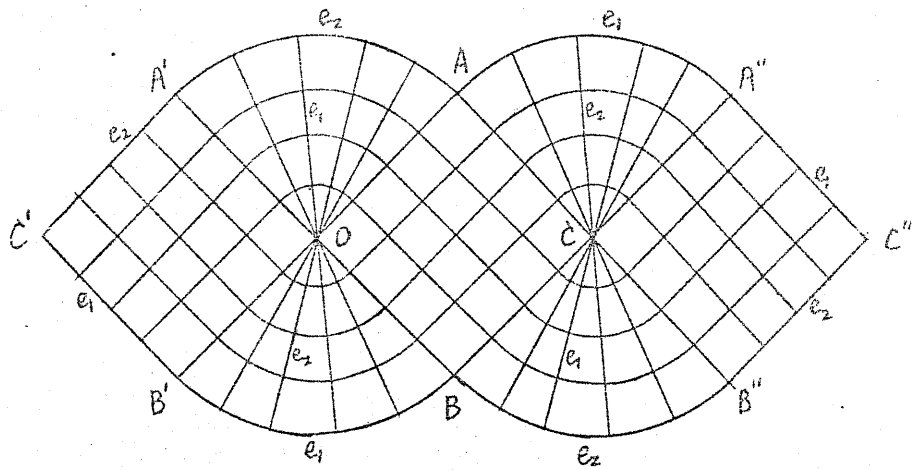


FIG. 9

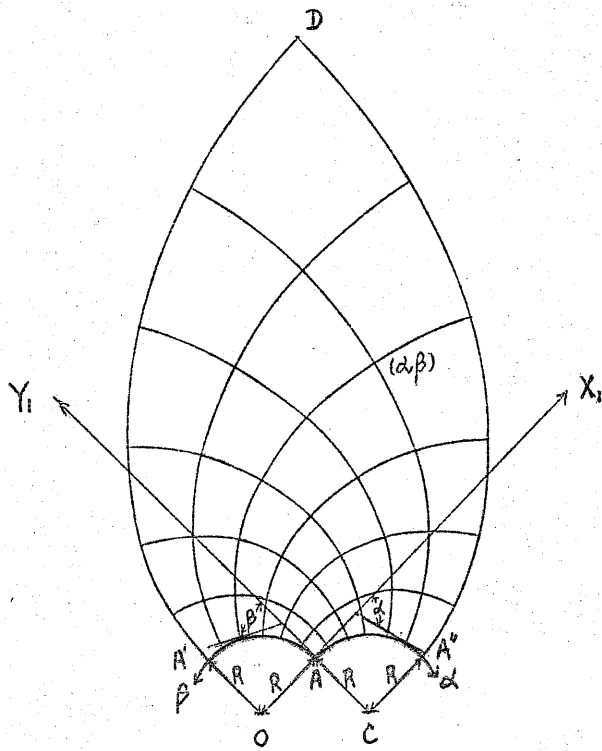


FIG. 10



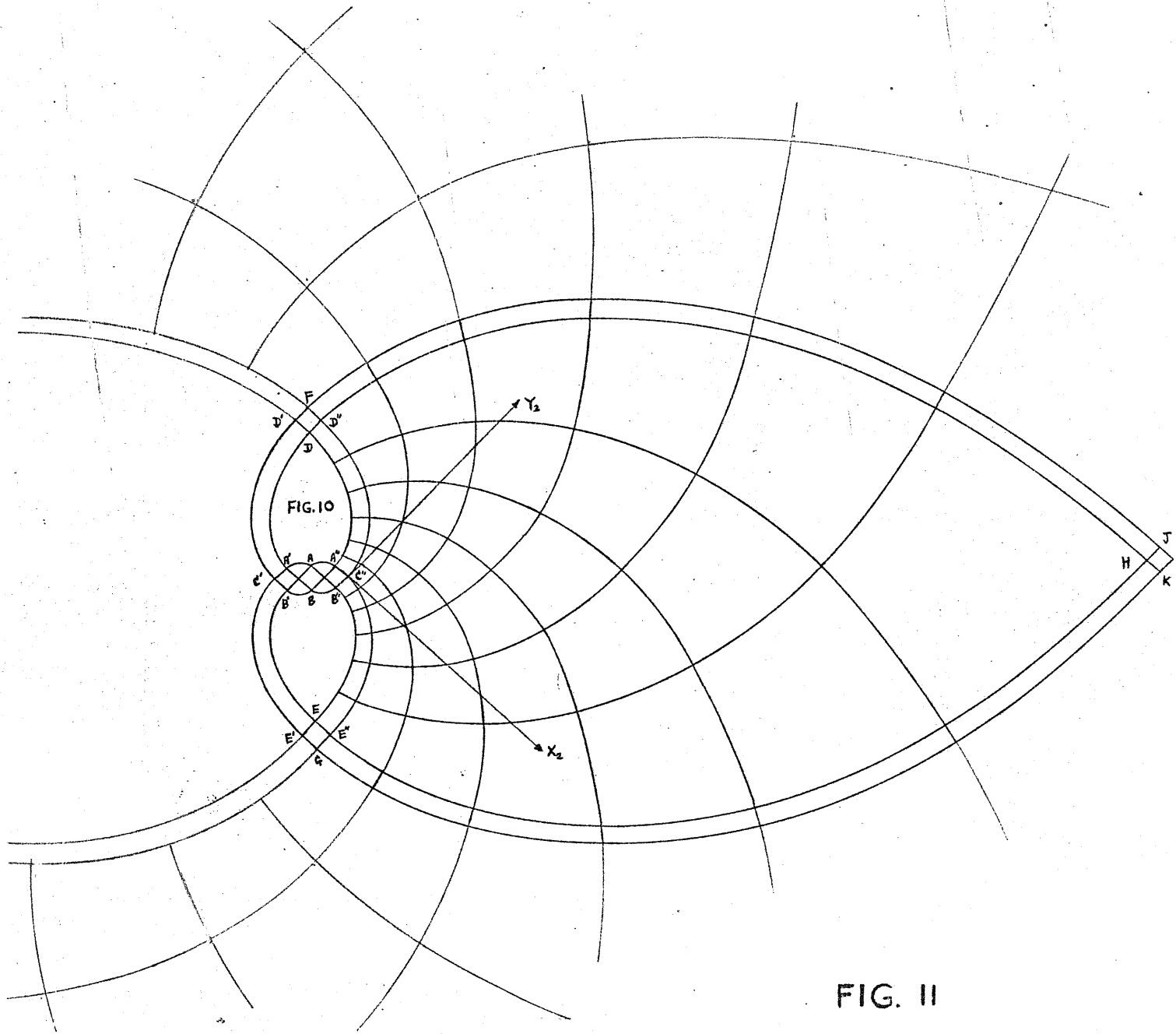


FIG. 10

FIG. II

FIG. 12

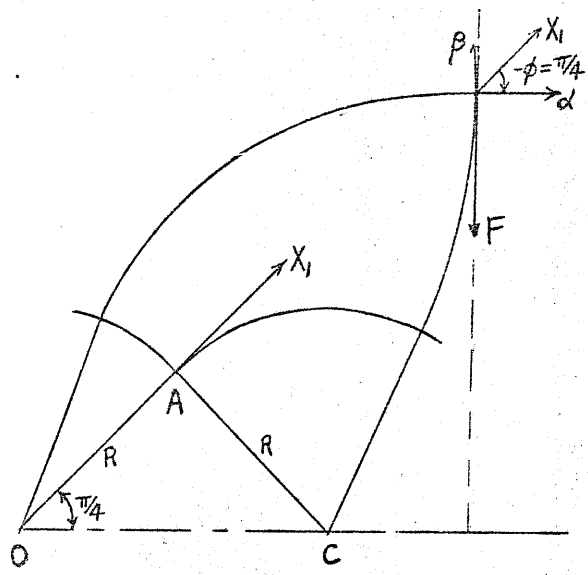
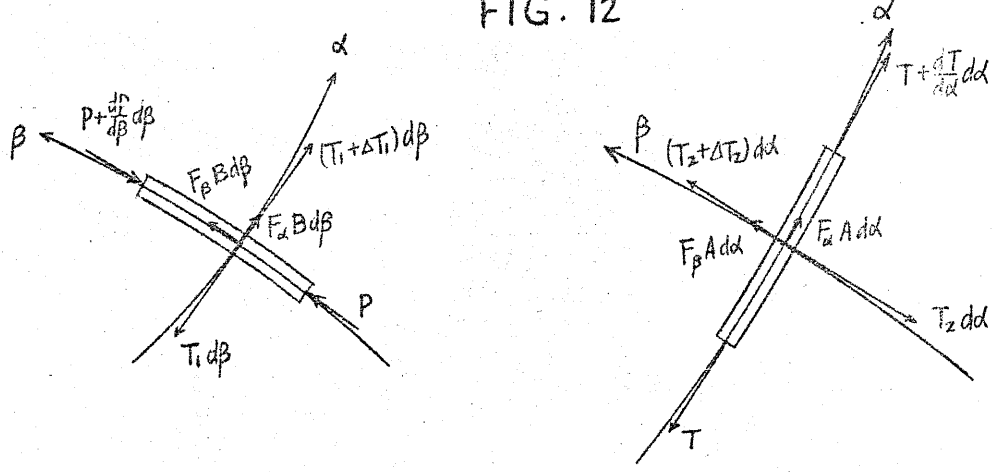
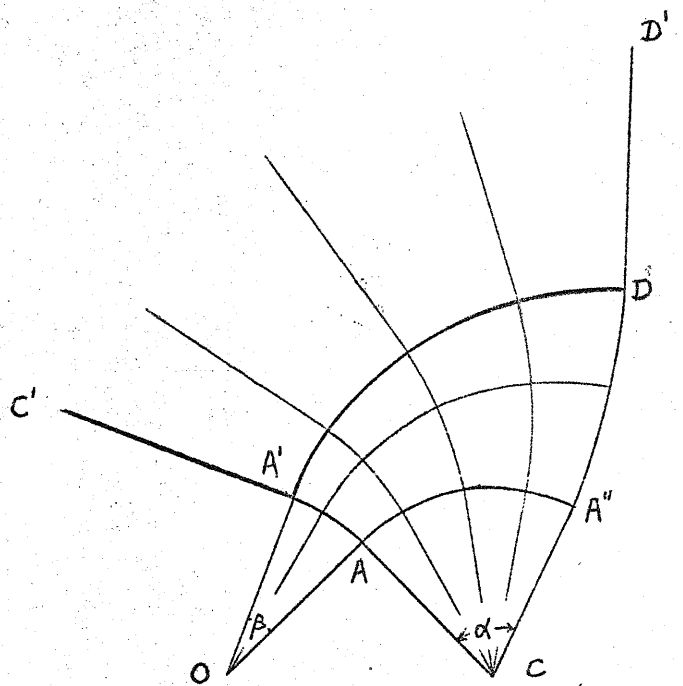


FIG. 14

FIG. 15

$$\alpha - \beta = \pi/4$$



A FORCE PERPENDICULAR TO THE LINE JOINING TWO FIXED SUPPORTS

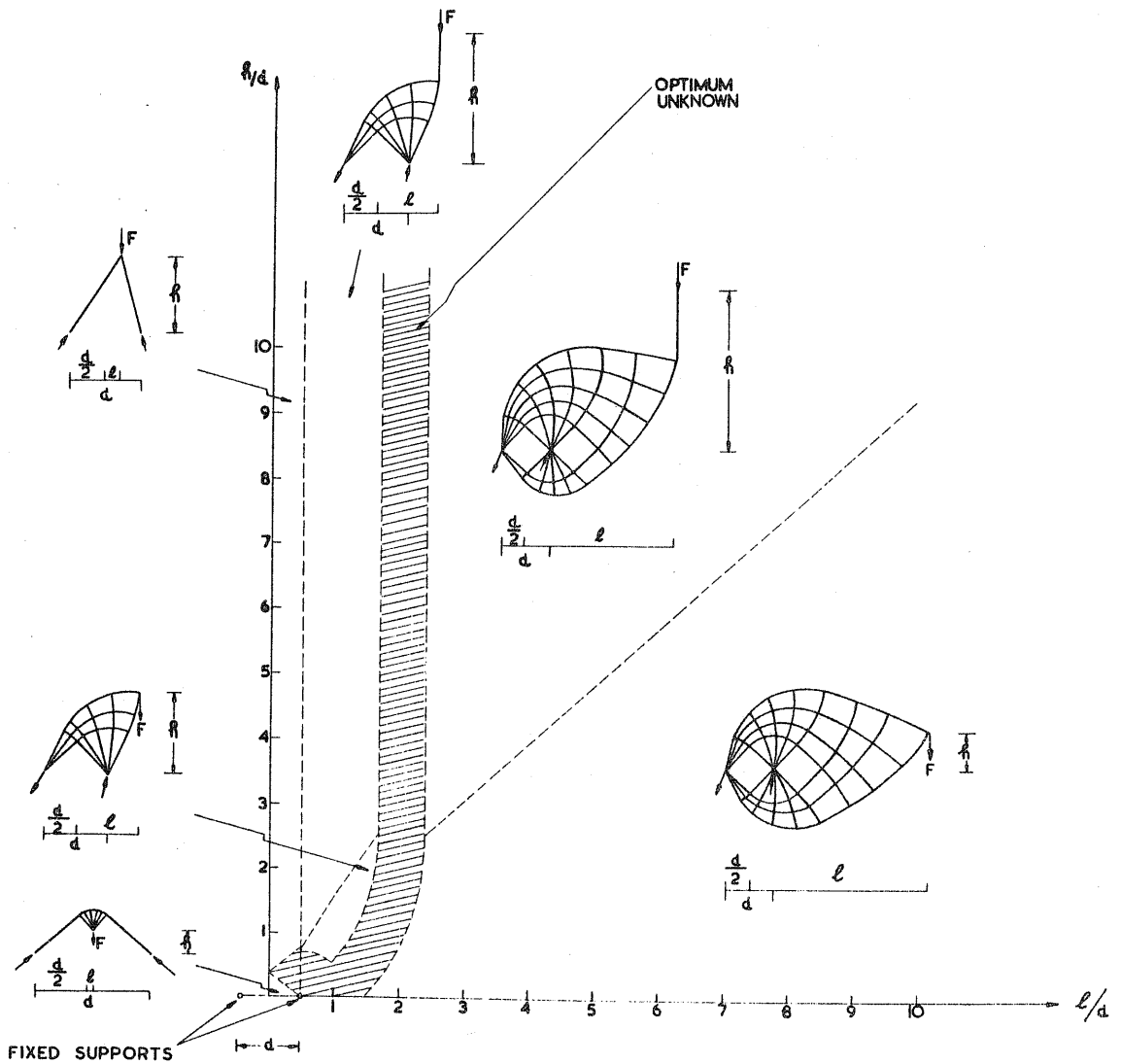


FIG.13a LAYOUTS OF OPTIMUM STRUCTURES
IN VARIOUS REGIONS

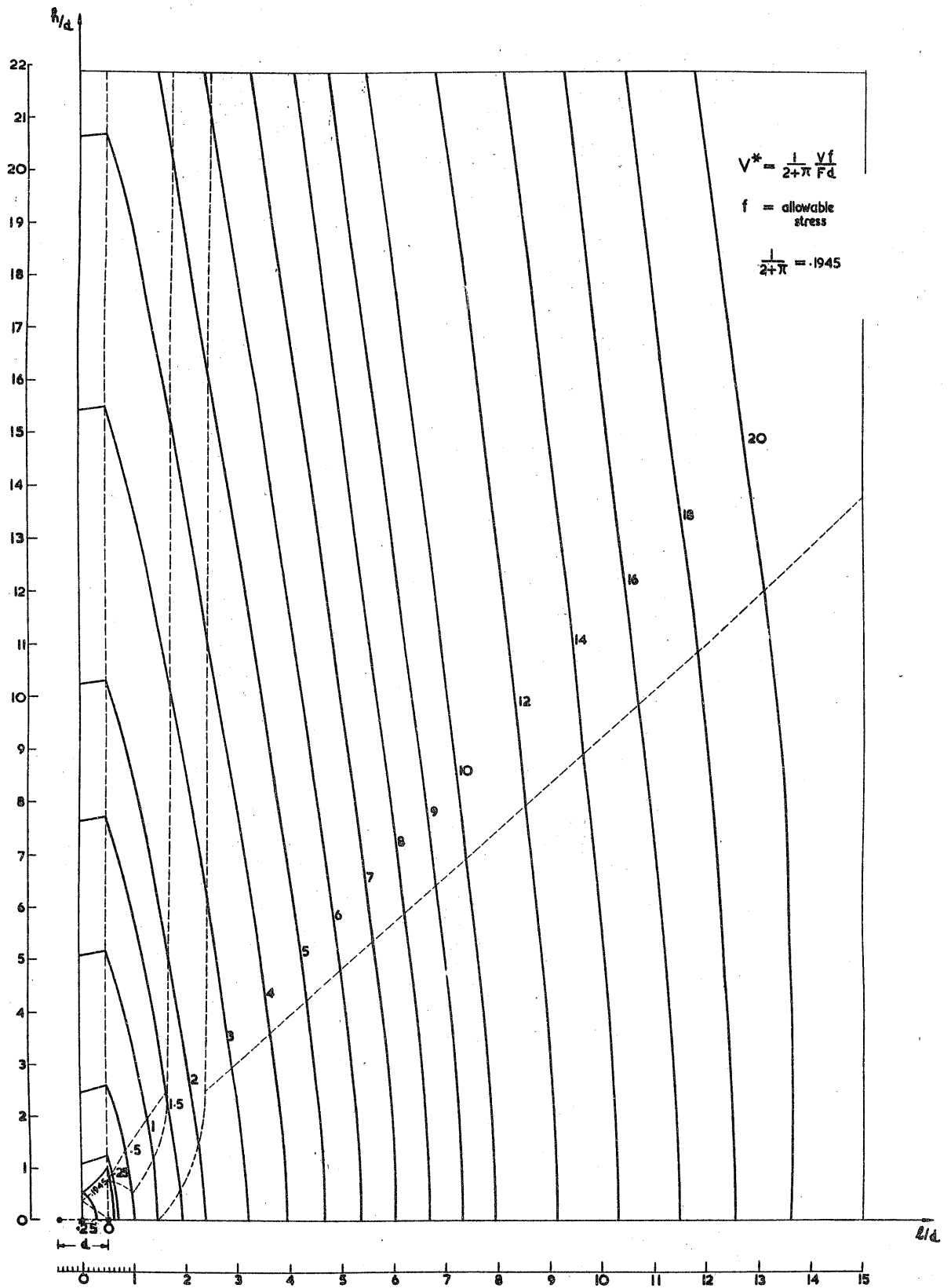


FIG.13b CONTOURS OF NONDIMENSIONAL VOLUME V^*

A FORCE PARALLEL TO THE LINE JOINING TWO FIXED SUPPORTS

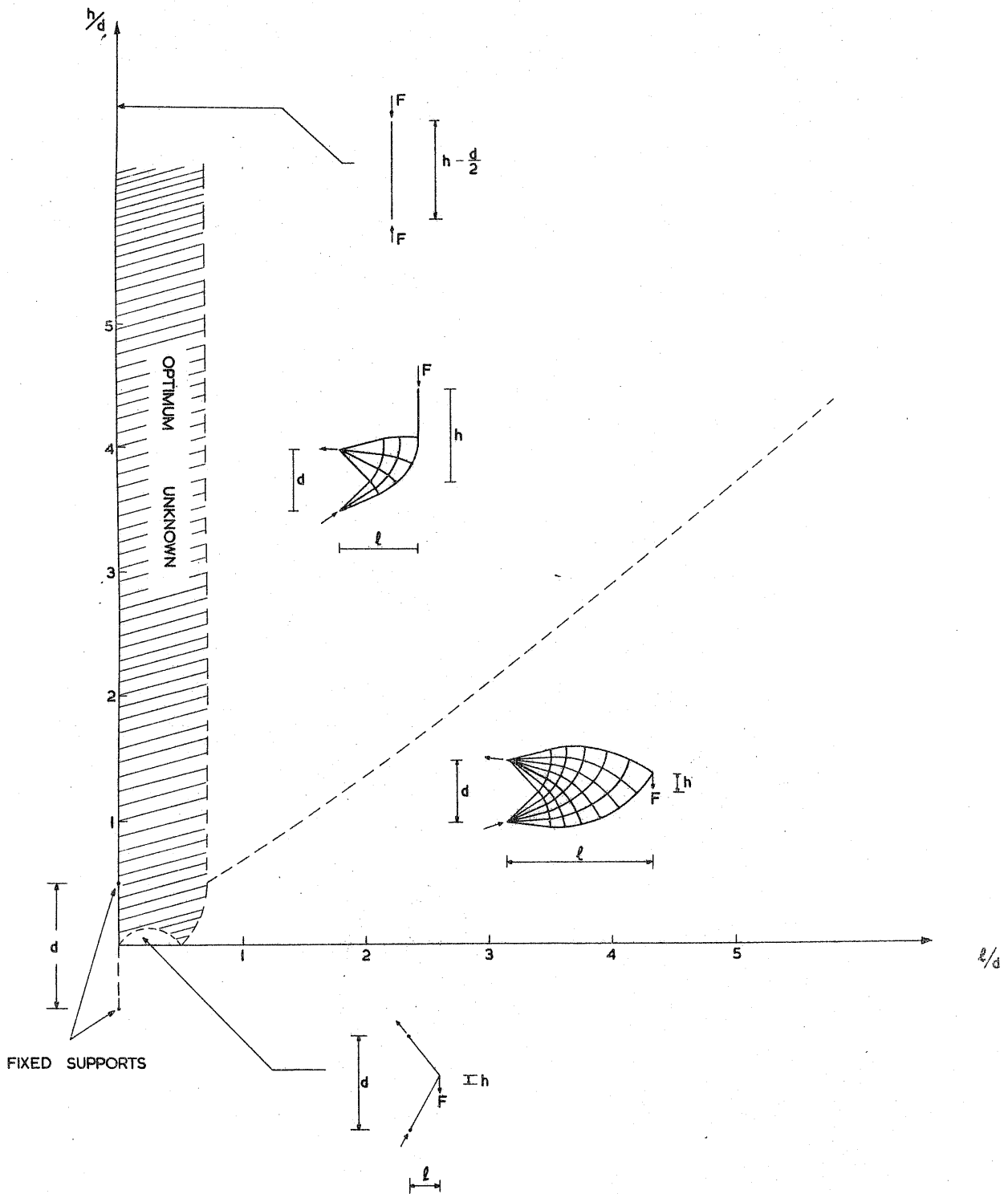
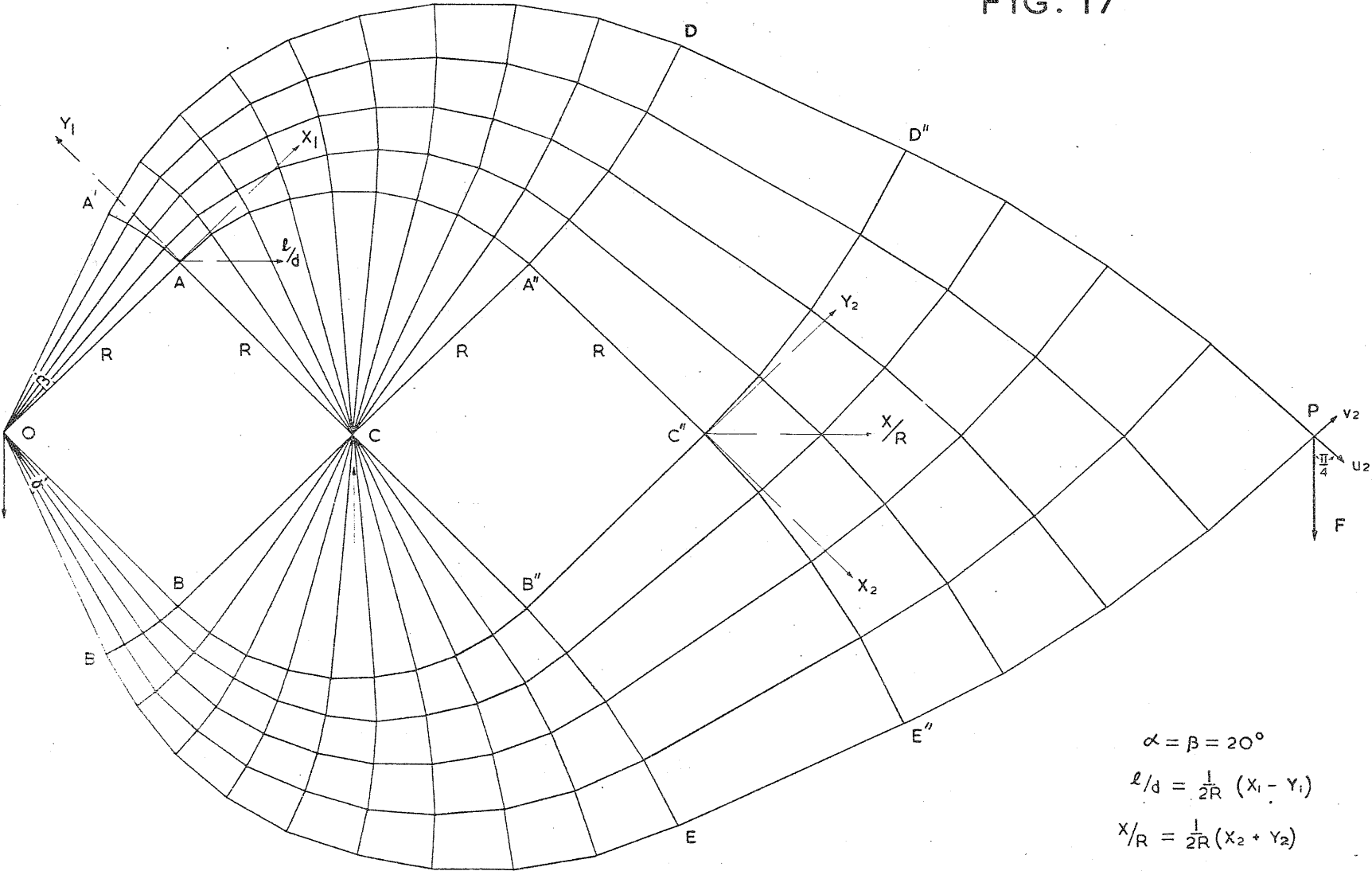


FIG. 16a LAYOUTS OF OPTIMUM STRUCTURES
IN VARIOUS REGIONS

FIG. 17



$$\alpha = \beta = 20^\circ$$

$$l/d = \frac{1}{2R} (X_1 - Y_1)$$

$$X/R = \frac{1}{2R} (X_2 + Y_2)$$

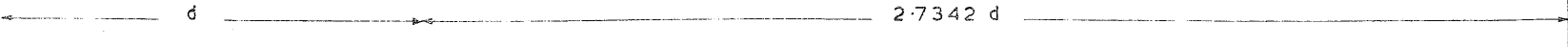
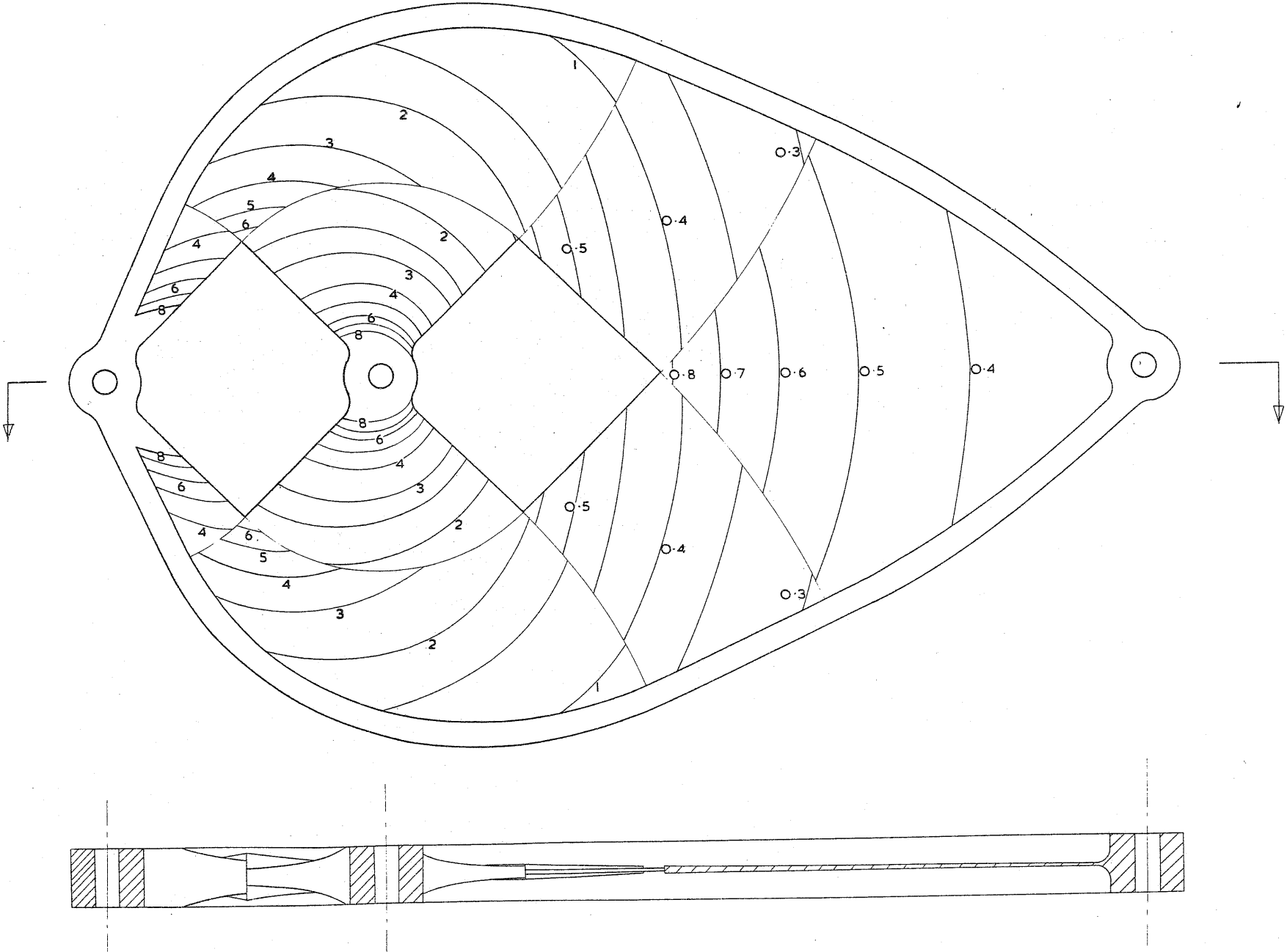


FIG. 18



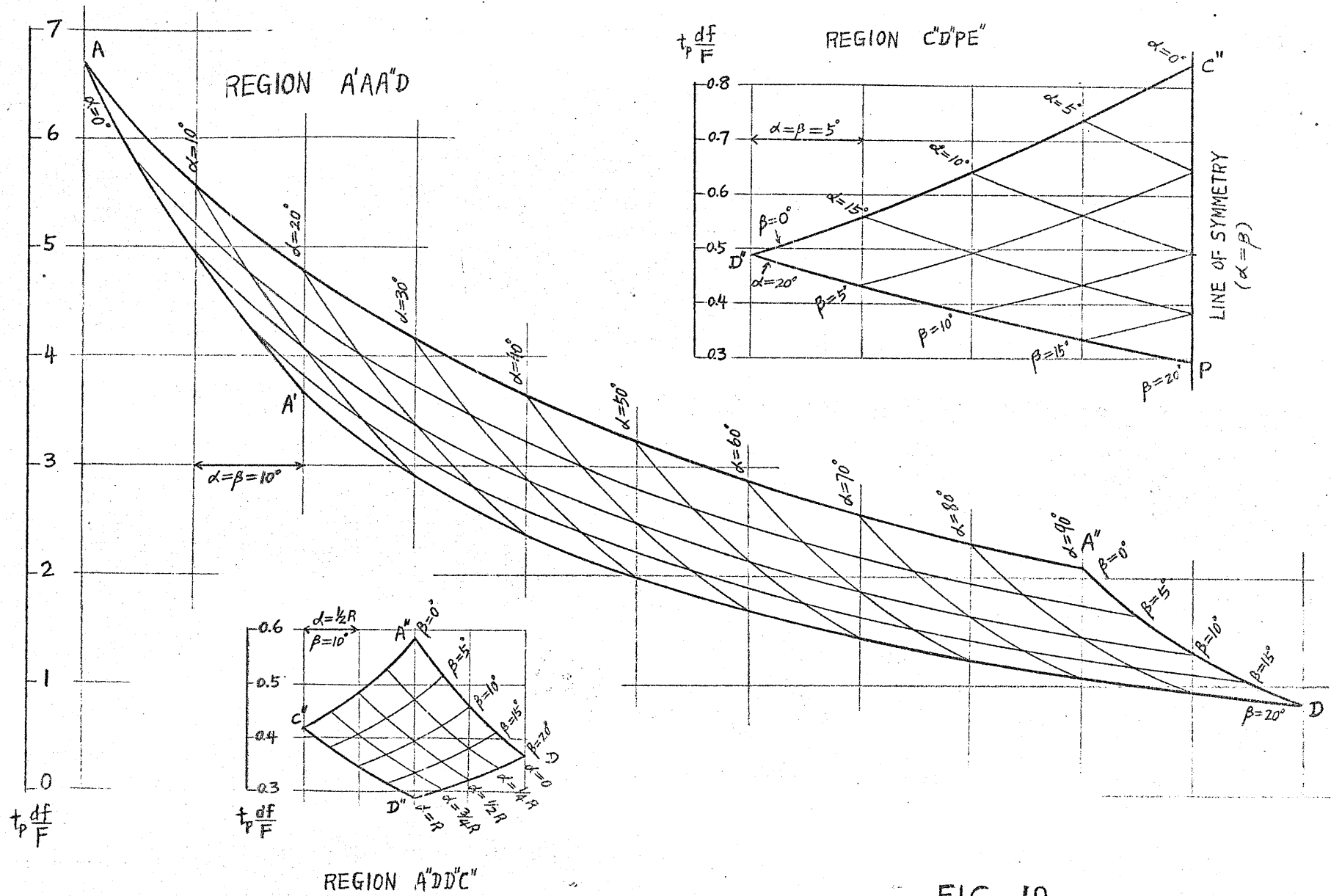


FIG. 19

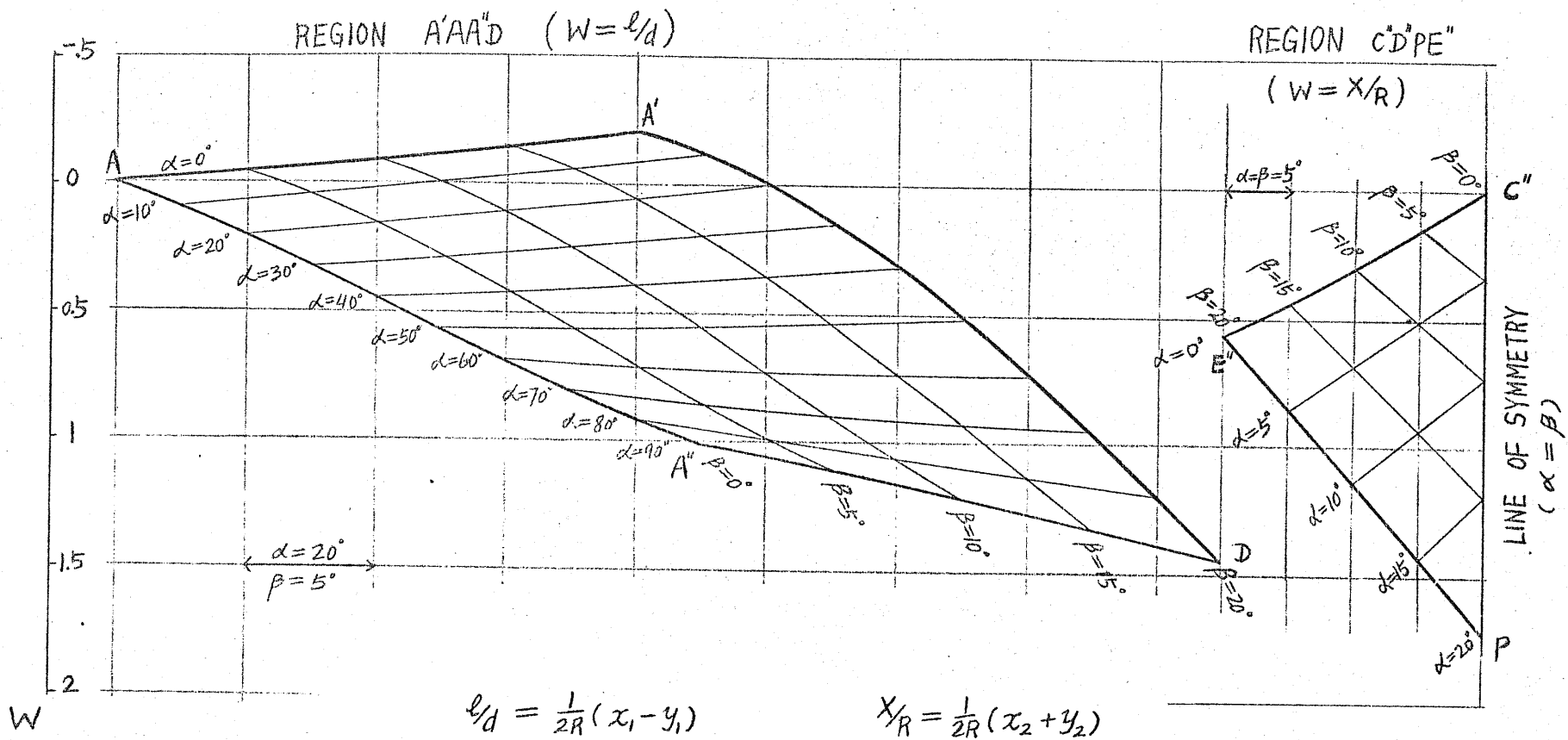


FIG. 20

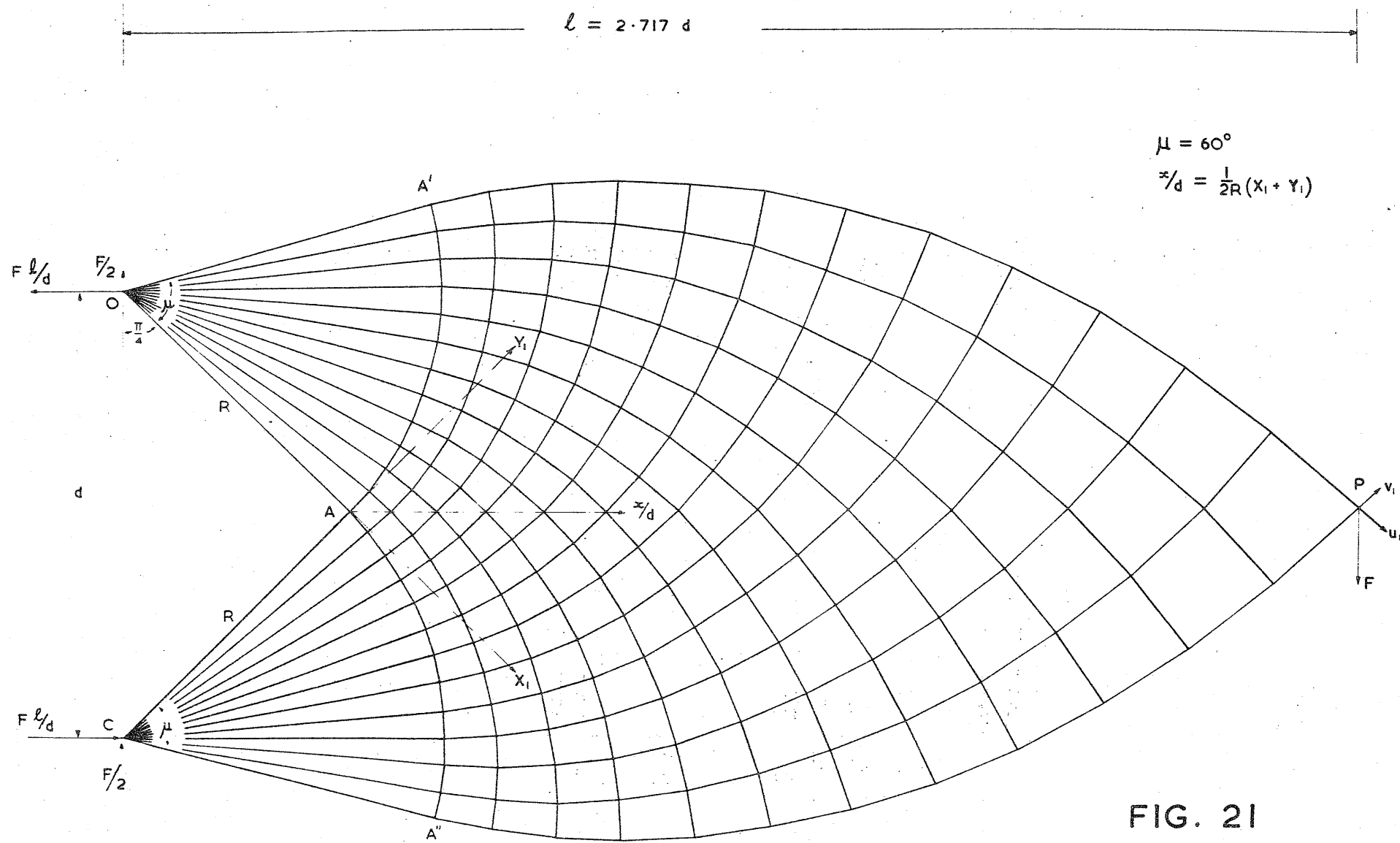


FIG. 21

FIG. 22

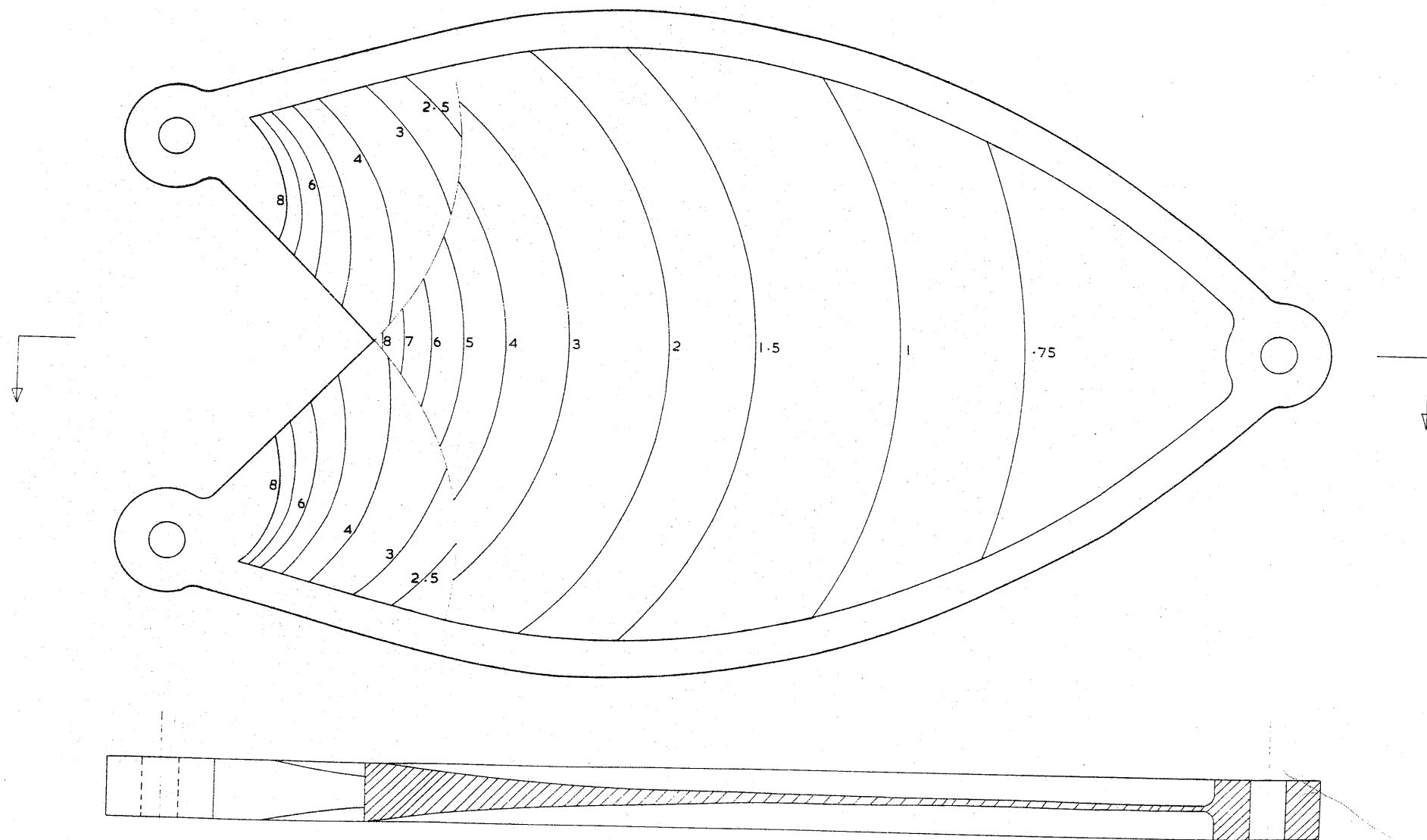
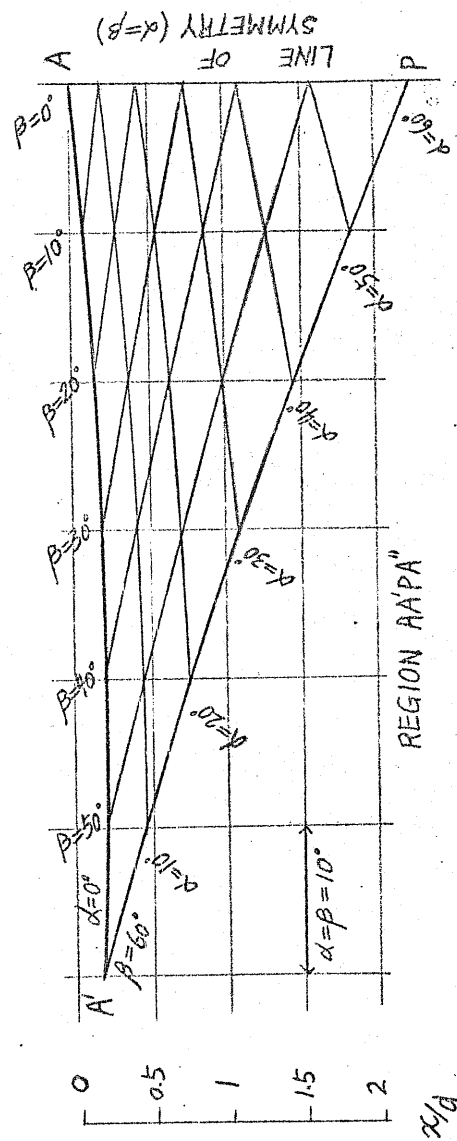
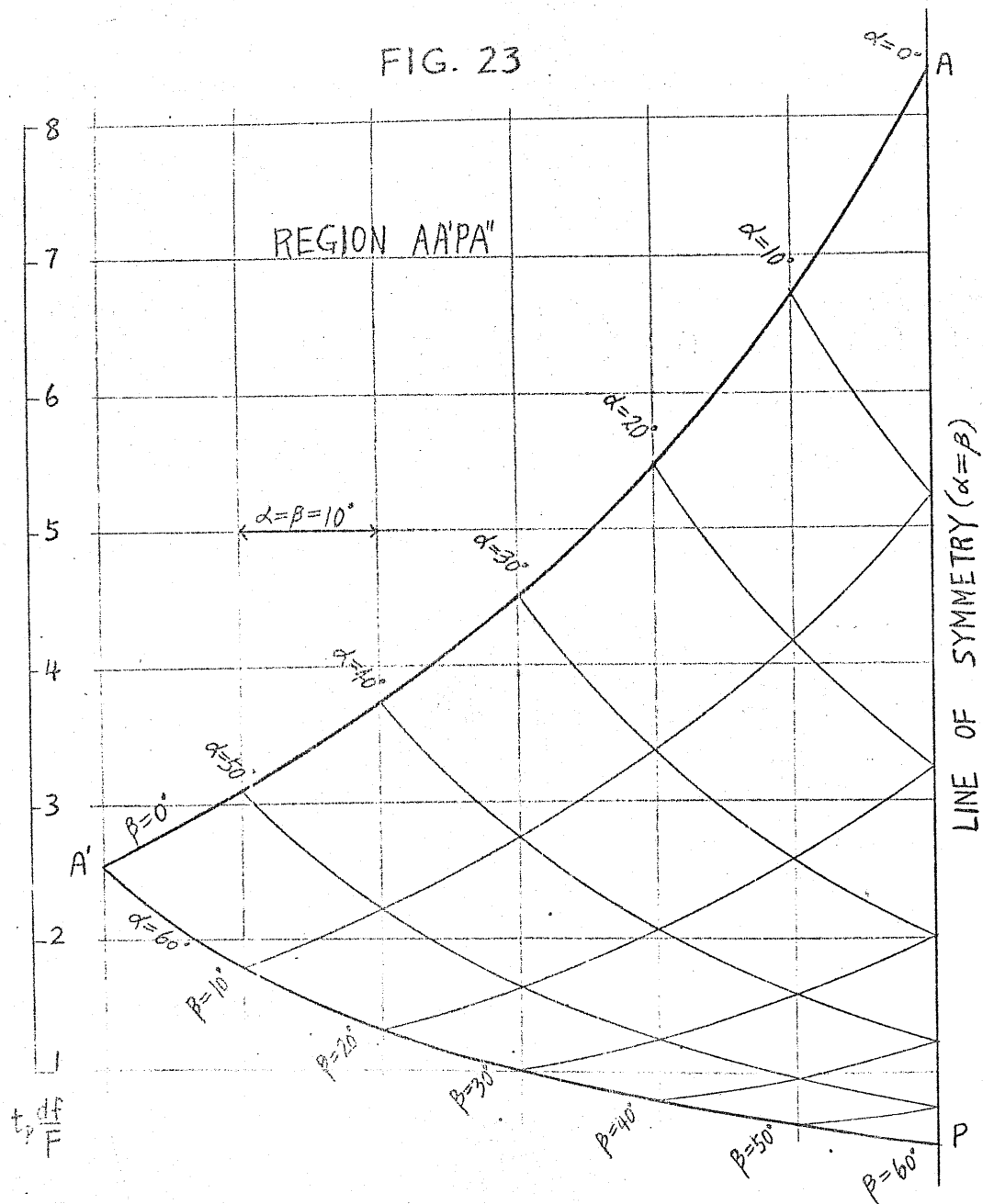


FIG. 23

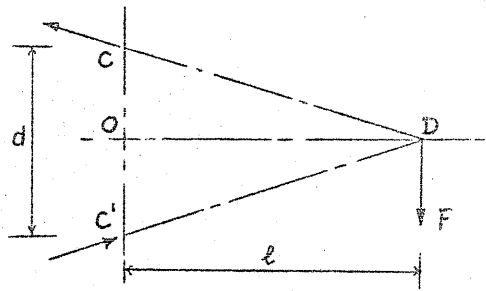


$$(1 + \frac{1}{x}) \frac{dF}{F} = \frac{1}{x} \frac{dF}{F}$$

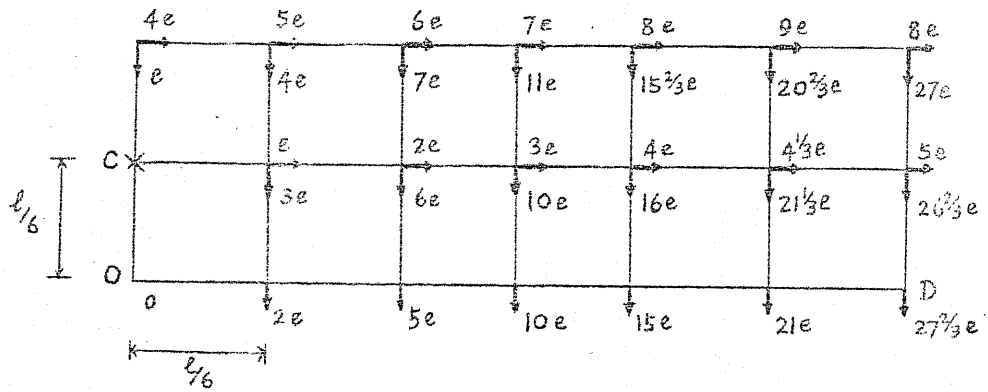
FIG. 24

FIG. 25

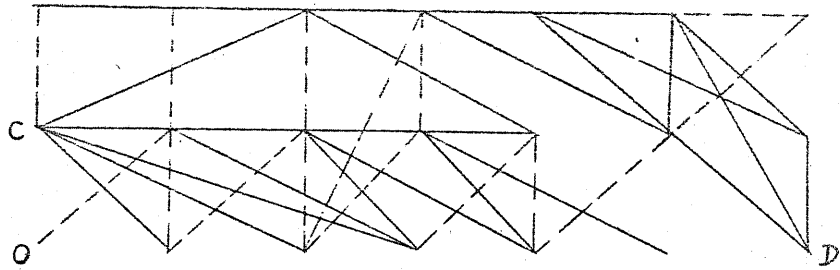
(a)



(b)



(c)



— MEMBERS WITH STRAIN e
 - - - MEMBERS WITH STRAIN $-e$

(d)

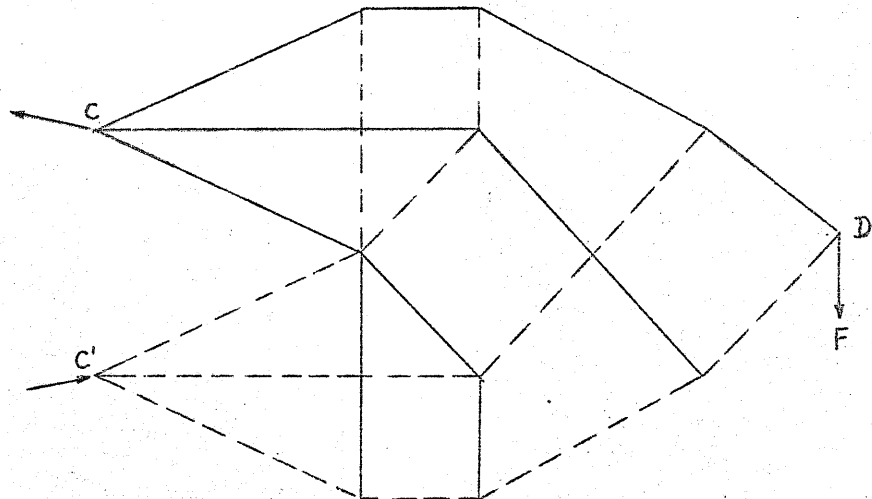
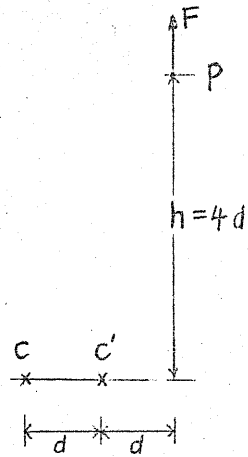
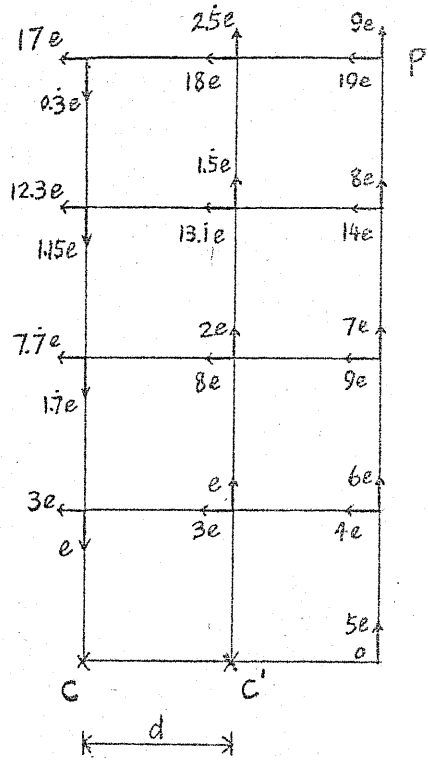


FIG. 26

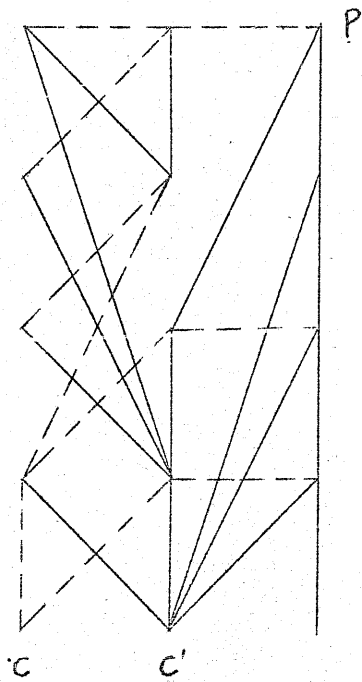
(a)



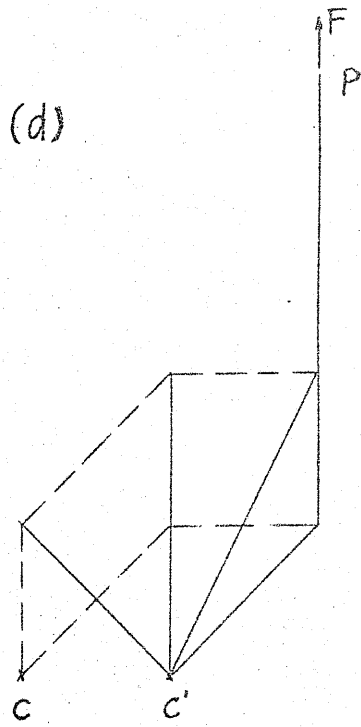
(b)



(c)



(d)



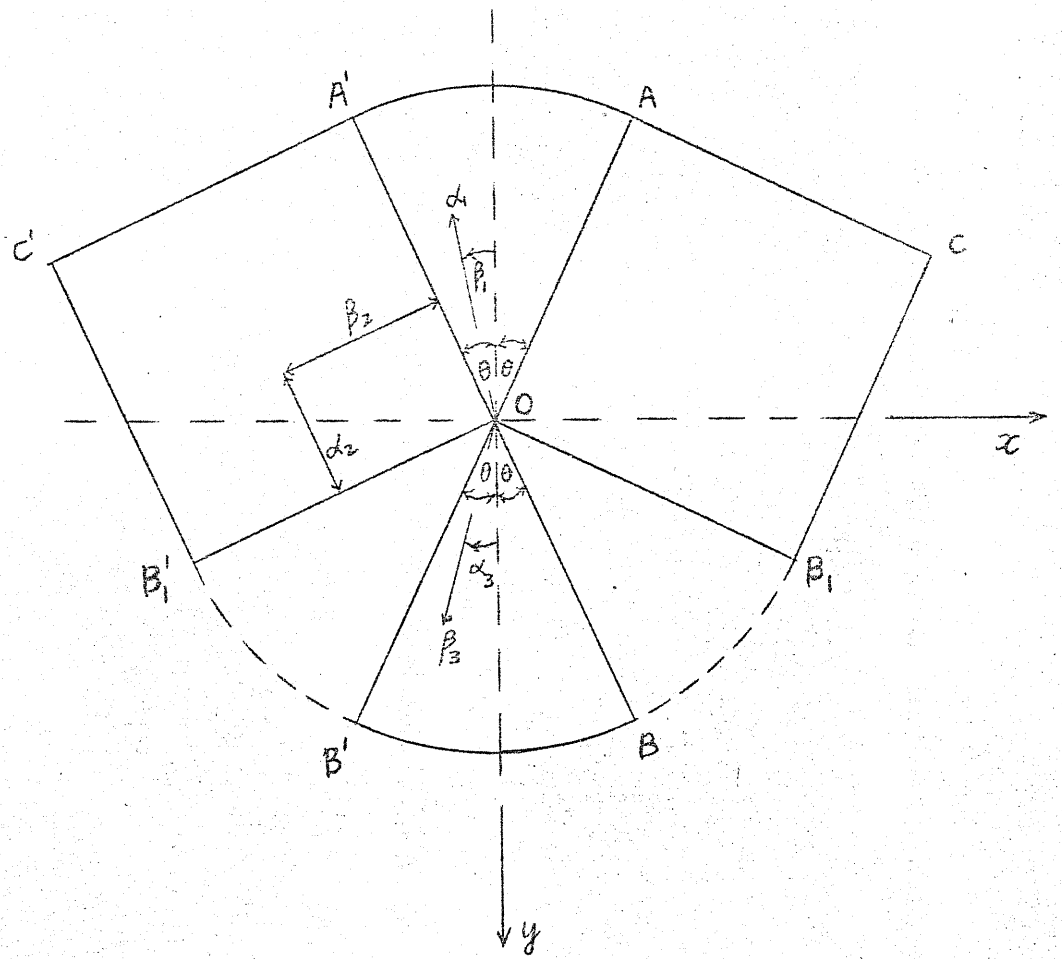


FIG. 27